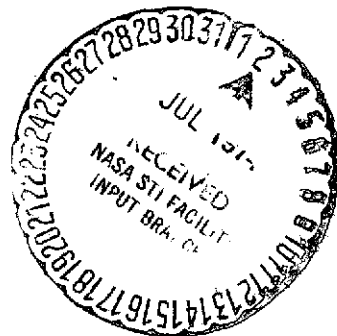


249

UNIVERSITY OF ARKANSAS

Graduate Institute of Technology

Department of Electronics and Instrumentation



Technical Report

GENERATION AND FLUID DYNAMICS OF
SCATTERING AEROSOLS IN LASER DOPPLER VELOCIMETRY

National Aeronautics and Space Administration

NASA CR-138657

(Grant NGL-04-001-007) FLUID DYNAMIC
STUDIES ON SCATTERING AEROSOL AND ITS
GENERATION FOR APPLICATION AS TRACER
PARTICLES IN SUPERSONIC FLOW MEASUREMENTS
(Arkansas Univ.) ~~54~~ p HC \$5.75 CSCL 20D

52

M74-26796

Unclas
G3/12 41285

A Technical Progress Report

for

work performed under

NASA Research Grant NGL 04-001-007
Ames Research Center
Moffett Field, California

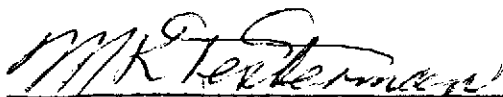
for that portion of the work entitled

FLUID DYNAMIC STUDIES ON SCATTERING AEROSOL AND
ITS GENERATION FOR APPLICATION AS TRACER PARTICLES IN
SUPERSONIC FLOW MEASUREMENTS UTILIZING LASER DOPPLER VELOCIMETER

by

M. K. Mazumder, B. D. Hoyle and K. J. Kirsch

Department of Electronics and Instrumentation
University of Arkansas Graduate Institute of Technology
Little Rock 72203



M. K. Testerman
Principal Investigator

April 22, 1974

TABLE OF CONTENTS

CHAPTER	PAGE
SUMMARY	1
I. INTRODUCTION	2
II. EQUATION OF MOTION OF A SMALL SUSPENDED PARTICLE	4
A. Particle-Fluid Interaction	4
B. Tracking Fidelity of Aerosols in an Oscillatory Flow Field	8
C. Motion of a Particle in an Acoustic Field	11
III. GENERATION OF A MONODISPERSE AEROSOL	13
A. Aerosol of Submicron Liquid Droplets	14
B. Aerosols of Monodisperse Solid Particles	15
IV. EXPERIMENTAL RESULTS	16
A. Experimental Setup	16
B. Frequency Response of Aerosols	17
C. LDV Signal Demodulation	20
V. CONCLUSIONS	21
VI. REFERENCES	21
TABLE 1	24
FIGURES	

LIST OF FIGURES

FIGURE

1. DECREASE OF ENERGY SPECTRUM RATIO $E_p(\omega)/E_g(\omega)$ WITH INCREASING TURBULENCE FREQUENCY AS A FUNCTION OF PARTICLE SIZE d_p
2. TYPICAL RMS TURBULENT VELOCITY COMPONENTS OF SUBSONIC FLUID FLOW IN A WIND TUNNEL ($\bar{U}_0 = 300$ m/sec) AND THE CALCULATED REYNOLDS NUMBER OF A UNIT DENSITY SPHERICAL PARTICLE PLOTTED AS A FUNCTION OF TURBULENCE FREQUENCY
3. MAXIMUM VALUES OF THE TURBULENCE FREQUENCY AND THE DIAMETER OF UNIT DENSITY SPHERICAL SCATTERER FOR TWO ENTRAINMENT FACTORS, $v_p/u_g = 0.707$ or $\omega\tau_p = 1$ and $v_p/u_g = 0.980$ or $d_p\sqrt{\omega} = 0.02$.
4. CALCULATED VARIATION OF THE FLUID VELOCITY AMPLITUDE (u_g) AND THE ASSOCIATED PARTICLE REYNOLDS NUMBER IN AN ACOUSTIC FIELD PLOTTED AS A FUNCTION OF ACOUSTIC INTENSITY LEVEL.
5. CUMULATIVE TYPICAL SIZE DISTRIBUTION CURVE FOR DOP AEROSOL GENERATED BY LASKIN ATOMIZER
- 5a. A PHOTOMICROGRAPH OF DOP AEROSOL GENERATED BY A LASKIN ATOMIZER (LINEAR MAGNIFICATION = 2090X)
6. RAPAPORT-WEINSTOCK AEROSOL GENERATOR
7. A PHOTOMICROGRAPH OF DOP AEROSOL GENERATED BY RAPAPORT-WEINSTOCK GENERATOR USING A 25 PERCENT CONCENTRATION OF DOP (LINEAR MAGNIFICATION = 2090X)
- 7a. A PHOTOMICROGRAPH OF DOP AEROSOL GENERATED BY RAPAPORT-WEINSTOCK GENERATOR USING A 5 PERCENT CONCENTRATION OF DOP (LINEAR MAGNIFICATION = 2090X)
8. POLYSTYRENE LATEX PARTICLE AEROSOL GENERATOR
9. A PHOTOMICROGRAPH OF 0.500 MICRON-DIAMETER POLYSTYRENE LATEX AEROSOL (LINEAR MAGNIFICATION = 2090X)
- 9a. A PHOTOMICROGRAPH OF 1.011 MICRON-DIAMETER POLYSTYRENE LATEX AEROSOL (LINEAR MAGNIFICATION = 2090X)
10. AN EXPERIMENTAL ARRANGEMENT FOR MEASURING THE FREQUENCY RESPONSE OF SCATTERING AEROSOL OSCILLATING IN AN ACOUSTIC FIELD
11. SCHEMATIC DIAGRAM OF A CIRCULAR PLATE RADIATOR (λ = WAVELENGTH OF SOUND IN THE RADIATOR MATERIAL)
12. ULTRASONIC INTENSITY LEVELS MEASURED AT A DISTANCE OF 3 CENTIMETERS FROM THE TOP OF THE RADIATING PLATE AS A FUNCTION OF EXCITATION FREQUENCY INPUT VOLTAGE 600 VOLTS PEAK-TO-PEAK, RESONANCE FREQUENCY = 37.8kHz.

13. RESPONSE OF A POLYDISPERSE DOP AEROSOL ($\sigma_g > 2.0$, AVERAGE DIAMETER 1.03 MICRONS, CONCENTRATION $\approx 10^7$ PARTICLES/cc) IN ACOUSTIC FIELDS
14. RESPONSE OF A POLYDISPERSE DOP AEROSOL ($\sigma_g > 2.0$, AVERAGE DIAMETER 1.03 MICRONS, CONCENTRATION $\approx 10^7$ PARTICLES/cc) IN ACOUSTIC FIELDS. PARTICLE SIZE RANGE: 0.3 - 2.0 MICRONS
15. POLYDISPERSE DOP AEROSOL RESPONSE IN ACOUSTIC FIELDS MEASURED BY A DISA 55L20 DOPPLER SIGNAL PROCESSOR
16. FAIRLY MONODISPERSE DOP AEROSOL ($\sigma_g \approx 1.4$, AVERAGE DIAMETER = 0.6 MICRONS, CONCENTRATION $\approx 10^6$ PARTICLES/cc) RESPONSE IN ACOUSTIC FIELDS
17. MONODISPERSE POLYSTYRENE AEROSOL ($\sigma_g \approx 1.0$, PARTICLE DIAMETER = 1.01 MICRONS, CONCENTRATION $\approx 10^5$ PARTICLES/cc) RESPONSE IN ACOUSTIC FIELDS
18. MONODISPERSE POLYSTYRENE AEROSOL ($\sigma_g \approx 1.0$, PARTICLE DIAMETER = 0.50 MICRONS, CONCENTRATION $\approx 10^5$ PARTICLES/cc) RESPONSE IN ACOUSTIC FIELDS
19. MONODISPERSE POLYSTYRENE AEROSOL ($\sigma_g \approx 1.0$, PARTICLE DIAMETER = 0.17 MICRONS, CONCENTRATION $\approx 10^5$ PARTICLES/cc) RESPONSE IN ACOUSTIC FIELDS
20. COMPARISON OF EXPERIMENTALLY MEASURED AND THEORETICALLY CALCULATED VELOCITY AMPLITUDE RATIOS FOR MONODISPERSE PARTICLES IN THE SIZE RANGE OF 0.176 TO 2.02 MICRON-DIAMETER AND FOR THE FREQUENCY OF OSCILLATION IN THE RANGE 5 TO 85 kHz

GENERATION AND FLUID DYNAMICS OF
SCATTERING AEROSOLS IN LASER DOPPLER VELOCIMETRY

M. K. Mazumder, B. D. Hoyle and K. J. Kirsch

SUMMARY

An experimental study on the particle-fluid interactions of scattering aerosols was performed using monodisperse aerosols of different particle sizes for the application of Laser Doppler Velocimeters in subsonic turbulence measurements. Particle response was measured by subjecting the particles to an acoustically excited oscillatory fluid velocity field and by comparing the ratio of particle velocity amplitude to the fluid velocity amplitude as a function of particle size and the frequency of oscillation. Particle velocity was measured by using a Differential Laser Doppler Velocimeter. An aspirator type atomizer was used to generate aerosols from a dilute suspension of monodisperse polystyrene latex particles. A Rapaport-Weinstock generator was used to generate aerosols of DOP droplets. The test aerosols were fairly monodisperse with a mean diameter that could be controlled over the size range from 0.1 to 1.0 micron. Experimental results on the generation of a fairly monodisperse aerosol of solid particles and liquid droplets and on the aerosol response in the frequency range 100 Hz to 100 kHz are presented. The present study indicates that a unit density spherical scatterer of 0.3 micron-diameter would be an optimum choice as tracer particles for subsonic air turbulence measurements.

I. INTRODUCTION

In a transonic or supersonic flow field where the flow medium is seeded with a scattering aerosol for velocity measurement with a Laser Doppler Velocimeter, a considerable amount of velocity lag may exist between the fluid motion and the motion of the suspended particles. For example, in a high fluid acceleration in the diverging region of a supersonic wind tunnel or in a rapid deceleration zone across a normal shock front, the velocity lag of the seed particles acting as the light scatterer would cause an appreciable error in the measurement of the fluid velocity employing a Laser Doppler Velocimeter.^{1,2} The size, the concentration, and the physical characteristics of the scattering aerosol are of paramount importance in the application of a Laser Doppler Velocimeter to fluid turbulence measurements. In general, the upper size limit is determined by particle inertia, and the lower size limit is determined by the increasing Brownian motion and the molecular slip in addition to the decreasing light scattering cross-section as particle size decreases. A polydisperse aerosol may cause an instrumental spread of the measured velocity distribution since a wide spectrum of aerosol size would result in a wide distribution of particle velocity lags. Thus, the scattering aerosol should be fairly monodisperse in size. The particle concentration should be sufficiently low so as to produce a negligible perturbation on the flow field, yet the concentration should provide the necessary amount of data in order that meaningful results can be obtained within the time of measurement. The physical properties of particles should be such that the aerosol is fairly stable, non-corrosive, non-toxic, and compatible with the physical properties of the fluid medium and the flow dynamics. Further, particle deposition on the optical windows should be minimum or should create minimum light scattering from the windows. The rate of generation and the method of introduction of the aerosol to the flow

medium should be controllable.

The objectives of the present study are (1) to study different methods of generating aerosols having the desired physical properties, and (2) to characterize the behavior of aerosol particles in a flow field. Because of the nonlinear particle-fluid interactions involved, particularly when the particle Reynolds number is greater than one, emphasis is given to the experimental determination of the response of the particles in a gaseous flow field. An experimental study on the particle-fluid interaction may be performed by subjecting the seed particles to known sinusoidal fluid velocity fields or to known fluid velocity gradients. A possible method of generation of a known fluctuating or oscillatory flow field is the excitation of the fluid medium by a propagating acoustic field. The frequency response of a flow-borne particle can be measured by subjecting the particle to an acoustic field of known frequency. Since nonlinear couplings are involved, the particle response will be a function of the excitation frequency, particle Reynolds number, and particle relaxation time. The dynamic components of the acoustic accelerating force applied to the particle should correspond to the components of the fluid accelerating force that a particle will actually experience in the flow field to be investigated by using a Laser Doppler Velocimeter.

This report discusses briefly the motion of aerosol particles in an acoustic field and some of the experimental arrangements for the particle response studies. It also describes two methods of generating a fairly mono-disperse scattering aerosol suitable for flow seeding for air turbulence measurements using Laser Doppler Velocimeters. Experimental data on small amplitude particle response are presented.

II. EQUATION OF MOTION OF A SMALL SUSPENDED PARTICLE

A. Particle-Fluid Interaction

For a small free spherical rigid particle in a locally uniform flow field, the force balance can be written from Newton's second law

$$m_p(dV_p/dt) = F_D + F_e \quad (1)$$

where m_p is the mass of the particle, V_p is the particle velocity, F_D is the fluid resistance force, and F_e represents the summation of the forces acting on the particle other than the fluid resistance forces. Examples of the latter forces are: gravitational force, "buoyant" or "lift" force caused by pressure gradients as well as by the presence of a shear layer of fluid, thermal forces and electrostatic forces.³⁻⁵

The fluid resistance force F_D can be expressed as

$$F_D = C_D(1/2) r_p^2 \bar{\rho}_g (U_g - V_p) |U_g - V_p| \quad (2)$$

where C_D is the drag coefficient, r_p is the particle radius, $\bar{\rho}_g$ is the average value of the fluid density, U_g is the vectorial velocity of the fluid, and V_p is the vectorial velocity of the particle. The drag coefficient, C_D , is a function of the particle Reynolds number, Re , which is given by

$$Re = d_p V_{pg} \bar{\rho}_g / \bar{\eta} \quad (3)$$

where $V_{pg} = |U_g - V_p|$,

and $\bar{\rho}_g$ and $\bar{\eta}$ are the average values of density and viscosity of the fluid,

respectively, and d_p is the particle diameter.

For small Reynolds numbers, $Re < 1$, where the inertial forces are small in comparison with the viscous forces in the medium, C_D can be represented by³

$$C_D = 24/(ReC_c). \quad (4)$$

The above relationship indicates that the particle motion is in the Stokes' law regime. The term C_c represents the Cunningham correction factor given by

$$C_c = 1 + (2A\lambda_g/d_p) \quad (5)$$

where
$$A = 1.25 + 0.44 \exp(-1.09 d_p/2\lambda_g) \quad (6)$$

and λ_g is the mean free path of the gas molecules. For $700 \leq Re \leq 2 \times 10^5$, $C_D = 0.44$ as was shown by Newton. For intermediate Reynolds numbers, $1 < Re < 700$, several approximate empirical relationships are available^{1,2} which express C_D in terms of Re , and it becomes difficult to give an exact analytical description of the flow field.

If only one coordinate-component of U_g and V_p are considered, and are denoted by u_g and v_p , the equation of motion of a small spherical particle can be approximated in the following form:⁶

$$(dv_p/dt) + av_p = au_g + b(du_g/dt) + c \int_{t_0}^t \{(du_g/dt' - dv_p/dt')/(t - t')^{1/2}\} dt'$$

where
$$a = 36\bar{n}/\{(2\rho_p + \bar{\rho}_g)d_p^2\}$$

$$b = 3\bar{\rho}_g / (2\rho_p + \bar{\rho}_g)$$

and
$$c = 18(\bar{\rho}_g \bar{\eta} / \pi)^{1/2} / \{(2\rho_p + \bar{\rho}_g) d_p\}$$

Tchen⁶ solved this equation to obtain the ratio of the Lagrangian energy-spectrum function $E_p(\omega)$ for the particle to the Lagrangian-energy spectrum function for the fluid $E_g(\omega)$. The relationship can be expressed as

$$E_p(\omega)/E_g(\omega) = \{1 + f_1(\omega)\}^2 + f_2^2(\omega) \quad (8)$$

where
$$f_1(\omega) = \frac{\omega(\omega + c\sqrt{\pi\omega/2})(b - 1)}{(a + c\sqrt{\pi\omega/2})^2 + (\omega + c\sqrt{\pi\omega/2})^2}$$

$$f_2(\omega) = \frac{\omega(a + c\sqrt{\pi\omega/2})(b - 1)}{(a + c\sqrt{\pi\omega/2})^2 + (\omega + c\sqrt{\pi\omega/2})^2}$$

ω is the angular frequency of turbulence components, and the constants a , b , and c are defined as above. Figure 1 shows the variation of $E_p(\omega)/E_g(\omega)$ as a function of turbulence frequency for unit density spherical particles of 1.0 and 0.3 micron-diameter calculated from Equation (8).

When the particle Reynolds number $Re < 1$, and $\rho_p \gg \bar{\rho}_g$, the terms containing the constants b and c in Equation (7) can be neglected. Thus, if the particle motion is in the Stokes' law regime, Equation (8) can then be simplified as follows

$$E_p(\omega)/E_g(\omega) = 1/(1 + \omega^2 \tau_p^2) \quad (9)$$

Where τ_p is the dynamic relaxation time⁷ of the particle which can be expressed as

$$\tau_p = (1/a)C_c = \rho_p d_p^2 C_c / 18\bar{\eta} \quad (10)$$

The term C_c , the Cunningham correction factor, becomes significant when d_p is smaller than or comparable to λ_g , the molecular mean free path. The mean free path increases significantly as the flow approaches the free molecular regime in high mach number flows.⁸

Equations (8) and (9) are based on linear fluid resistance law. In a low-Reynolds-number flow, the fluid resistance force is given by Stokes' law, i.e.,

$$F_D = 6\pi\bar{\eta}r_p(v_p - u_g) \quad (11)$$

and the heat transfer between the gas and a single particle⁹ is

$$Q_p = 4\pi r_p k(T_p - T_g) \quad (12)$$

where k is the thermal conductivity of the gas, T_p and T_g are the instantaneous temperatures of the particle and of the surrounding fluid respectively.

Equations (11) and (12) are valid for a spherical particle moving with uniform velocity at a low Reynolds number in a viscous fluid. In most actual turbulent flow cases, temperature, density and dynamic viscosity of the fluid are variables and the fluid resistance force becomes nonlinear.

Motion of suspended particles in an oscillating fluid can be studied by subjecting the aerosol to an acoustic plane wave. Since the energy of turbulence in a fluid flow is distributed over a spectrum of frequencies, experiments carried out at discrete frequencies can be related to the motion of particles in a turbulent fluid if the fluid turbulence conditions are simulated. Since nonlinear fluid resistance forces are involved, both

amplitude and frequency of the fluctuating fluid velocity field under test conditions should be comparable to the turbulent velocity components over the spectrum of frequencies.

Figure 2 illustrates typical values of root mean square turbulence velocity components as a function of frequency of turbulence in a subsonic wind tunnel.^{10,11} The mean velocity is approximately 300 meters per second. Curve No. 1, shown as an unbroken line, represents turbulent velocity components in a wind tunnel of throat area approximately 30 cm X 30 cm. Curve No. 2, shown as an unbroken line, represents similar quantities for isotropic turbulence in a 25 cm-diameter wind tunnel. The curves shown in broken lines represent corresponding rms Reynolds numbers of a spherical, unit density, one micron-diameter particle suspended in the fluid medium. The fidelity of seeded particles in tracking the fluid velocity fluctuations in such a flow field can be experimentally determined by measuring the ratio of the particle velocity amplitude to the fluid velocity amplitude while the particles are in an oscillatory flow field of comparable velocity amplitude at the frequency of excitation.

B. Tracking Fidelity of Aerosols in an Oscillatory Flow Field

The equation of motion of a particle of radius r_p in an oscillatory flow field can be written in the form⁷

$$m_p (dv_p/dt) = -6\pi\eta r_p (v_p - u_g) \quad (13)$$

$$+ 6\pi\eta r_p (\omega r_p^2 / 2\bar{\nu})^{1/2} \left[(u_g - v_p) + (1/\omega) d(u_g - v_p)/dt \right. \\ \left. + (2/3\omega) (\omega r_p^2 / 2\bar{\nu})^{1/2} (du_g/dt) \right]$$

where $\bar{\nu}$ is the kinematic viscosity of the gas and ω is the angular frequency

of oscillation. The second term of Equation (13) represents deviation from Stokes' law regime. If the nonlinear terms in Equations (7) and (13) are to be made negligible, the following constraints must be satisfied:

$$\begin{aligned}
 \omega\tau_d &\leq 1 \\
 (\omega r_p^2 / 2\bar{\nu})^{1/2} &\ll 1 \\
 (\bar{\rho}_g / \rho_p) &\ll 1 \\
 \sigma_g &\leq 1.5 \\
 Re &\ll 1 \\
 K_n &< 0.2 \\
 m_p n / \rho_g &< 0.01
 \end{aligned}
 \tag{14}$$

Under these conditions of linear particle-fluid interactions, a high tracking fidelity of a flow borne aerosol in a subsonic flow field can be assumed.

The above conditions are not mutually independent but do set criteria relating to the physically meaningful quantities. The first three criteria imply that the flow is in Stokes' regime. These conditions also imply that the dynamic relaxation time τ_p and thermal relaxation time τ_T of the particle are small. The latter quantity is given by

$$\tau_T = P_r c_p' r_p^2 / 3\bar{n} c_p \tag{15}$$

where P_r is the Prandtl number which is equal to $c_p \bar{n} / k$, c_p' is the specific heat of the particle, c_p is the specific heat of gas at constant pressure and k is the thermal conductivity of the gas. The fourth condition implies that the seeded aerosol should be fairly monodisperse and the standard

deviation of the particle size spectrum is close to one. Because of inherent difficulties in generating a true monodisperse aerosol and because of the inherent unstable nature of aerosols, a maximum value for the standard deviation (σ_g) of 1.5 is chosen as a practical limit. A larger value of σ_g may cause appreciable error in turbulence measurement because of the possible wide distribution of particle velocity lags. The fifth constraint is satisfied in most actual subsonic flow cases where $r_p < 2$ microns, $\rho_p = 1$ gram/cc and the frequency of turbulence does not exceed 100 kHz. Figures 1 and 2 indicate that for $d_p = 1$ micron, the gas-particle relative velocities and rms Reynolds numbers remain small in subsonic turbulence. The requirement that the Knudsen number ($K_n = \lambda_g/d_p$) be smaller than 0.2 implies that for air at STP, $d_p > 0.3$ microns, so that the molecular slip is small. The last constraint indicates that particulate mass loading ratio is small; thus the perturbation of the flow field will be negligible. The lower limit of particulate mass loading is set by the Doppler signal dropouts.

In discussing the above constraints, it was assumed that the scattering particles are uncharged, inert, and are not volatile in the surrounding fluid.

Figure 3 shows the calculated maximum values of the frequency of the oscillating flow field and of the diameter of unit density spherical scatterers for $v_p/u_g = 0.707$ ($\omega\tau_d = 1.0$) and for $v_p/u_g = 0.980$ ($d_p\sqrt{\omega} = 0.02$). Assuming that a tracking fidelity of 98 percent is desired in a turbulence measurement where the spectral components do not exceed 100 kHz, $d_p\sqrt{\omega} = 0.02$, and $f = 10^5$ Hz, the value of the particle diameter, d_p , is 0.25 microns for 98 percent fidelity. Considering the constraints in Equation (14) that $K_n < 0.2$, i.e., $d_p > 0.3$ microns for air at STP, a possible optimum choice of tracer particle diameter would probably be 0.3 microns with $\rho_p = 1.0$ for air turbulence measurements.

C. Motion of a Particle in an Acoustic Field

When the constraints given in Equation (14) are satisfied, the motion of an oscillating particle in an acoustic field, can be written in the form

$$\tau_p (dv_p/dt) + v_p = u_g \sin \omega t \quad (16)$$

Equation (16) represents one dimensional motion of a particle in an acoustic field of angular frequency ω . Equation (16) has a solution in the form

$$v_p = \{u_g \sin(\omega t + \phi)/(1 + \omega^2 \tau_p^2)^{1/2}\} + \{\tau_p u_g \omega/(1 + \omega^2 \tau_p^2)\} e^{-t/\tau_p} \quad (17)$$

where the phase shift ϕ is given by

$$\phi = \tan^{-1} \omega \tau_p \quad (18)$$

The second term of Equation (17) represents the transient response of the particle. When $t \gg \tau_p$, we can write the steady state solution for the ratio of the amplitude of the particle velocity to the amplitude of the fluid velocity as

$$(v_p/u_g) = 1/(1 + \omega^2 \tau_p^2)^{1/2} \quad (19)$$

The ratio (v_p/u_g) is often referred to as the degree of entrainment and is denoted by μ_p . Equation (19) indicates that the fidelity with which an aerosol particle follows the fluid motion increases with decreasing particle

diameter, density, and excitation frequency and with increasing viscosity of the medium.

The velocity amplitude of an element of fluid subjected to an acoustic plane wave of intensity I in watts/meter², is given by

$$u_g = (2I/\bar{\rho}_g c_g)^{1/2} \quad (20)$$

where c_g is the velocity of the propagating acoustic wave. The amplitude of displacement is given by

$$A_g = u_g/\omega \quad (21)$$

where ω is the angular frequency of excitation. Since acoustic intensity levels are generally measured in terms of dB referred to 10^{-12} watts/meter², the intensity level IL is given by

$$IL = 10 \log_{10} \frac{I \text{ in watts/m}^2}{I_0 \text{ in watts/m}^2} \text{ re } I_0 \text{ watts/m}^2 \quad (22)$$

where $I_0 = 10^{-12}$ watts/meter². Figure 4 shows calculated relationships between acoustic intensity levels in dB and fluid velocity amplitude u_g (solid line). The velocity amplitude, v_p , of a suspended particle can be calculated from Equation (19). Using Equations (3) and (18) the particle Reynolds numbers were calculated for $d_p = 1, 5$ and 10 microns; $\rho_p = 1.0$ gram/cc; and $f = 10$ and 100 kHz. The calculated values of Re are plotted in Figure 4 (broken lines). Air at 760 mm Hg at 20°C is assumed as the fluid medium.

Several experimental verifications of Equation (19) have been attempted^{12,13}

most of which employed determination of the amplitude of particle oscillation using photographic means. Although there was general agreement between the experimental data and the expected particle response, the experimental results scatter widely and the validity of the analysis was more qualitative than quantitative. A Laser Doppler Velocimeter provides an excellent method of measurement of suspended particle response in acoustic fields.

In Figure 4, a linear coupling of acoustic excitation with the medium is assumed. In practice, the waveform of the propagating wave becomes distorted at a distance from the source, particularly when the acoustic intensity is high. If nonlinear terms in particle-fluid interaction are present, particle motion may become further distorted. However, the approximate values of the particle Reynolds numbers plotted in Figure 4 indicate that the acoustic intensity level required to subject an aerosol (with $d_p = 1$ micron, $\rho_p = 1.0$ gram/cc) to a value of $Re \geq 1$ would be very high. Several particle difficulties limit the generation of such a highly intense acoustic field in gases. However, an oscillatory flow field of high velocity amplitude can be established in a resonant air column such as a siren tuned cavity, Galton whistle, etc.

Particle-fluid interaction with a particle Reynolds number $Re > 1$, may be realized in the following flow conditions: (1) particles suspended in a fluid acceleration field passing a throat, (2) flow of particles through a standing shockwave, where particles experience a large deceleration field and (3) propagation of a shockwave through a stationary fluid medium containing particles.

III. GENERATION OF A MONODISPERSE AEROSOL

Two of the most desirable features of seed particles in Laser Doppler

Velocimeters are that (1) the particles must be an efficient scatterer at the wavelength of laser radiation and (2) flow tracking fidelity must be high. As discussed in the earlier section, a monodisperse submicron aerosol of solid particles or of liquid droplets seems to satisfy these requirements. Liquid droplets of very low vapor pressure have an advantage over the solid particles in that their deposition on the optical windows results in a formation of a liquid film that does not cause a severe light scattering problem from the window surfaces. Since aerosol coagulates spontaneously, the coagulated liquid droplets remain spherical. However, solid particles with a high melting point must be used where temperatures of the fluid medium are high.

A. Aerosol of Submicron Liquid Droplets

Laskin-type atomizers¹⁴ can be used to generate DOP ($\rho = 0.98$; refractive index, $m = 1.4$ at $\lambda = 5000\text{\AA}$; vapor pressure = 1.48×10^{-7} mm Hg at 25°C) aerosol as well as Dow Corning 200 Silicone fluid ($\rho = 0.96$; $m = 1.4$ at $\lambda = 5000\text{\AA}$; viscosity 50 and 100 centistokes) aerosols. As a rule, pneumatic atomization produces a polydisperse mist. A typical cumulative size distribution of DOP aerosol¹⁵ produced by a Laskin atomizer is shown in Figure 5. Figure 5A shows a typical photomicrograph of a sample of the aerosol generated by the Laskin atomizer.

Generation of a monodisperse condensation aerosol using a heat-exchanger type generator¹⁶ is advantageous compared to the Laskin atomizer. A Rapaport-Weinstock generator¹⁶ was used for generating fairly monodisperse DOP aerosols. Aerosols with mean diameter varying from 0.1 to 1.5 microns could be produced. A schematic diagram of the generator is shown in Figure 6. A dilute solution of DOP in alcohol was atomized and the poly-

disperse mist was evaporated in the heated column. The vapor finally condensed on the impurity nuclei to form a monodisperse aerosol. By using different nozzle sizes and by controlling the dilution ratio of DOP to alcohol, the droplet size could be varied from 0.1 to 1.5 microns in diameter. Two typical photomicrographs of DOP aerosol are shown in Figures 7 and 7b. The droplets were electrostatically deposited on a microscope slide surface deactivated with 3M L-1668 chemicals. The standard deviation, σ_g , of the particle size distribution can be maintained below 1.5

B. Aerosols of Monodisperse Solid Particles

Monodisperse aerosols containing solid spherical particles were generated by atomizing an alcohol suspension of polystyrene latex spheres ($\rho_p = 1.05$, $m = 1.58$ at $\lambda = 5000\text{\AA}$). Uniform (one standard deviation within 0.005 microns) polystyrene latex particles in the size range 0.1 to 1.0 micron were used. These particles were obtained from Dow Diagnostics. The aerosol generator is shown in Figure 8. A lucite tube, 1/4" I.D. and 1/2" O.D., with 6 radial holes of 0.0135" diameter was used as an atomizer. The bottom end of the tube was closed. The open end was connected to a pressurized N_2 tank through a pressure regulator and an absolute filter. The radial holes were positioned so that the nitrogen gas jets skim the surface of the suspension. A dilute suspension was used to produce an aerosol in which most of the particles were singlets (latex particle). It was found that the latex particles in an alcohol suspension have less tendency to coagulate when the solution concentration is altered. Also, alcohol film on the particles evaporates faster than the water film. Thus an alcohol suspension was used in the latex particle aerosol generator. Figures 9 and 9a show two photomicrographs of the generated aerosol of 0.500

1.011 micron-diameter particles. The ratio of single particles to all other particles, such as doublets, triplets, etc. was found to be high.

IV. EXPERIMENTAL RESULTS

A. Experimental Setup

An experimental arrangement for the measurement of the frequency response of a scattering aerosol is shown in Figure 10. A 500 mW argon-ion laser beam of wavelength 4880A is incident on the outermost track of an encoder disc having a spatial frequency of 100 lines/mm. The disc is rotated at a sufficient speed by a synchronous motor to permit a frequency translation¹⁶ of 2 MHz of the Doppler signal. The test aerosol is suspended in an acoustic excitation chamber. Air at room temperature was used as the fluid medium. The fluid medium containing the aerosol was excited by acoustic horns. The frequency of excitation could be varied at discrete steps from 100 Hz to 100 kHz. The Doppler signal was demodulated by a phase-locked loop demodulator using a Signetics NE 561B PLL circuit. The acoustic pressure levels at the point of velocity measurements were measured by using a calibrated Bruel and Kjaer condenser microphone (1/4 inch diameter, Type 4135) followed by a preamplifier (B&K model 2618). The demodulated Doppler signal and the microphone output were displayed on a dual beam oscilloscope. Velocity amplitudes of u_g and v_p were calculated from the oscilloscope display.

Acoustic excitation in the frequency range below 15 kHz was carried out using loud speakers and tweeters. Sound pressure levels in the range of 100 to 120 dB were used at different resonant frequencies of the chamber. For the transmission of ultrasonic vibrations into the fluid medium, flexural vibrating plates were used. A typical transducer driven by a piezoelectric

crystal is shown in Figure 11. The transducer consists of a circular, flexurally vibrating, free-edge plate with stepped thicknesses. The plate is driven at its center and it can vibrate at several resonant frequencies corresponding to different flexural modes of vibration. A number of ultrasonic radiators were made with different resonant frequencies. The measured output acoustic levels in air at a distance of 3 cm from one of the ultrasonic radiators is shown in Figure 12.

During the acoustic excitation, standing waves in both longitudinal and transverse modes were formed. Since only a one-dimensional particle oscillation was measured with the Laser Doppler Velocimeter, a correction factor was needed for obtaining an exact coincidence of $v_p/u_g = 1.0$ for $d_p = 0.176$ microns at $f = 20$ kHz as is expected from Equation (19).

B. Frequency Response of Aerosol

The method of determining the particle response in an oscillatory fluid velocity field was as follows: The test aerosol was introduced inside the acoustic excitation chamber by connecting the input of the chamber to the aerosol generator while the other part of the chamber was connected to a vacuum line. After a suitable concentration of aerosol was obtained inside the chamber, both the ports were closed. The acoustic exciter was then energized and the acoustic pressure level at a point close to the laser beam crossing was measured by the microphone. The velocity oscillations of the aerosol were measured by the Laser Doppler Velocimeter. Both the modulating signal (microphone output) and the demodulated signal (Doppler signal processor output) were displayed on a dual beam oscilloscope. A sample of aerosol was taken from the chamber and its photomicrograph was analyzed to determine the aerosol size distribution. The process was repeated for each test aerosol.

Figures 13 through 19 show some typical oscilloscope displays of modulating and demodulated signals for different particle size and for different frequencies of acoustic excitation. Figures 13 and 14 show the response of a polydisperse DOP aerosol in acoustic fields. The aerosol was generated by a Laskin atomizer. As the modulating frequency increased from 5 kHz to 50 kHz, the velocity amplitudes of the aerosol showed a velocity distribution as is evident from the spread in amplitude of the displayed signal. Such a velocity spread is expected at high frequencies since the larger particles lag the smaller ones. Figure 15 shows a similar display of the response of a polydisperse DOP aerosol using DISA Type 55L35 Frequency Tracker as the Doppler signal demodulator. The tracker was obtained on loan from DISA Electronics, New Jersey, in order to determine whether or not the signal-to-noise ratio of the demodulated output can be further improved by using a frequency feedback system such as is used in the tracker. No improvement in SNR was observed compared to the phase-locked-loop system in the present application. A bandpass filter having a narrow bandwidth centered around the modulating frequency was found necessary for Doppler signal demodulation. In the present work, a phase-locked-loop FM demodulator and tunable bandpass filter were used for Doppler signal processing.

Figure 16 shows the response of a fairly monodisperse DOP aerosol at the modulation frequency of 20.84 and 51.46 kHz. The aerosol was generated by using the Rapaport-Weinstock aerosol generator. A comparison of Figure 16 with Figures 13 and 14 shows that the distribution of velocity lag is much narrower in the case of the DOP aerosol generated by the Rapaport-Weinstock aerosol generator. The narrower size distribution of the aerosol is also evident from the photomicrograph shown in Figure 7A when the same is compared with the size distribution shown in Figure 5A.

Figures 17 through 19 show the response of monodisperse aerosols in acoustic fields. The distribution of velocity lag for such test aerosols was found negligible which also indicates that the aerosol particles are mostly singlets and the coagulation rate is small.

Acoustic excitation levels at the point of velocity measurement were maintained at a constant level for a given frequency of excitation. The particle velocity amplitudes for different size particles can thus be directly compared from the oscilloscope display of the demodulated signal. Thus the ratio of the velocity amplitudes was not affected by the attenuation of the acoustic wave caused by the presence of the aerosol. An appreciable attenuation was found when the mass loading ratio ($m_p n / \rho_g$) was high and the product $\omega \tau_p$ was close to one.

Table 1 shows the ratio of the measured particle velocity amplitude for the test aerosol to the measured particle velocity amplitude for particles of 0.176 micron-diameter ($\rho_p = 1.05$). The choice of 0.176 micron-diameter particles as a reference for u_g was made since these particles are expected to follow an oscillatory flow field without any appreciable velocity lag in the frequency range DC to 100 kHz. For example $v_p/u_g = 0.994$ for $f = 84.0$ kHz (from Equation 19). The relative amplitude ratio ($v_p/v_{0.176}$) was preferred since the measurement of u_g from the microphone output may have the following sources of error: (1) the microphone is not directional and thus it cannot measure the one dimensional component u_g alone if other orthogonal components are present, and (2) the size of the microphone becomes comparable to the wavelength of acoustic radiation at the higher frequencies. Figure 20 shows a plot of the theoretically calculated ratio of relative particle velocity amplitudes. Experimental data points show a close fit to the expected values.

Figure 21 shows the entrainment ratio (v_p/u_g) as a function of $r_p \omega^{1/2}$

(a factor related to the square root of the nondimensional frequency $\omega\tau_p$). In this figure, the experimental data were taken for $d_p = 0.176, 0.500, 0.760$ and 1.011 microns polystyrene particles and for $f = 8.56, 37.80, 58.00$ and 82.80 kHz. In this experiment a different horn was used for acoustic excitation. Although the 0.176 micron-diameter particles follow the velocity fluctuations with a high fidelity, the optimum choice would probably be 0.30 micron-diameter tracer particles because of the larger light scattering crosssection of 0.3 micron particles.

The average acoustic intensity level at the point of velocity measurement was approximately 120 dB which corresponds to a value of $u_g = 5.5$ cm/sec. Thus the experimental data presented here are strictly valid for low amplitude oscillation of particle velocity. However, if the velocity amplitude is increased further to simulate the expected turbulence component as shown in Figure 2, the constraints of Equation (14) would still be valid. As a result no appreciable departure from the results shown in Figures 20 and 21 is expected. An experimental verification of particle fidelity under simulated conditions close to the actual turbulent flow field is now underway.

C. LDV Signal Demodulation

During the present experiments, it was observed that laser Doppler signal processing at a modulating frequency above a few kHz becomes a difficult problem. Doppler signal demodulators, used in the present work, show that when the frequency (f) of a fluid velocity oscillation is increased above a certain value, the output SNR of the signal degrades to a point where no meaningful data can be taken. The degradation of output SNR is probably caused by the fact that as f is increased the modulation index $\beta(\Delta f/f)$ decreases and the output SNR ($\text{SNR} \propto \beta^2$) decreases. When the SNR is below the threshold value of FM demodulation, the performance of the analog

tracking systems becomes very poor. The degradation is further accentuated by signal dropouts. SNR can be improved significantly if the frequency of oscillation is known. In such a case a narrow bandpass filter can be used to filter the noise outside the pass band. A tunable bandpass filter was used in the present set of experiments. In actual turbulence analysis, the processor must have a demodulated signal bandwidth DC to 100 kHz. A digital counter type or a photon correlator type of Doppler signal demodulator may be suitable in such applications.

V. CONCLUSIONS

An analysis of the particle-fluid interaction and scattering properties of the aerosol indicates that a fairly monodisperse aerosol of 0.3 micron-diameter is an optimum choice for tracer particles in subsonic turbulence studies employing a Laser Doppler Velocimeter. Experimental results presented here seem to confirm this analysis. Methods of generating a submicron aerosol for flow seeding of inert gases at ambient temperature are discussed and experimental data are presented.

VI. REFERENCES

1. Yanta, W. J., "Turbulence Measurements with a Laser Doppler Velocimeter," Naval Ordnance Laboratory Report NOLTR 73-94, May 1973.
2. Berman, N., "Particle-Fluid Interaction Corrections for Flow Measurements with a Laser Doppler Flowmeter," NASA Report N73-23379, 1969.
3. Hidy, G. M. and Brock, J. R., Topics In Current Aerosol Research, Pergamon Press, N.Y., 1971.

4. Friedlander, S. K., "Behavior of Suspended Particles in a Turbulent Fluid," AICHE Journal 3, 381 (1957).
5. Soo, S. L., Fluid Dynamics of Multiphase Systems, Blaesdell Publishing Co., Waltham, Mass., 1967.
6. Hinze, J. O., Turbulence, McGraw-Hill Book Co., N.Y., 1959.
7. Fuchs, N. A., The Mechanics of Aerosols, McMillan Co., N.Y., 1964.
8. Lapp, M., Penny, C. M., and Asher, J. A., "Application of Light-Scattering Techniques for Measurement of Density, Temperature, and Velocity in Gas Dynamics," Aerospace Research Laboratories Report ARL-73-0045, April 1973.
9. Brock, J. R., "On the Theory of Thermal Forces Acting on Aerosol Particles," J. Colloid Sc. 17, 768 (1962).
10. Seegmiller, H. L., Personal Communication, NASA Ames Research Center, California.
11. Laufer, J., NACA TR 1174 (1954).
12. Gucker, F. T. and Doyle, G., "The Amplitude of Vibration of Aerosol Droplets in a Sonic Field," J. Phys. Chem. 60, 989 (1956).
13. Brandt, O. and Hiedemann, E., "The Aggregation of Suspended Particles in Gases by Sonic and Supersonic Waves," Trans. Faraday Soc. 32, 1101 (1936).

14. Parrish, E. C. and Schneider, R. W., "Tests of High Efficiency Filters and Filter Installations at ORNL," Oak Ridge National Lab., ORNL-3422, June 1963.
15. Lowry, P. L., "Agglomeration of Dioctyl Phthalate Filter Tests Aerosols," M. S. Thesis, University of Arkansas, 1973.
16. Davies, C. N. (Ed), Aerosol Science, Academic Press, N.Y., 1966.
17. Mazumder, M. K., "Laser Doppler Velocity Measurement without Directional Ambiguity by Using Frequency Shifted Incident Beams", Appl. Phys. Letters, 16, 462 (1970).

TABLE 1

Correlation of Theoretically Calculated and
Experimentally Observed Velocity Amplitude Ratios
(Note: $v_{0.176}/u_g = 0.994$ @ 84 kHz)

Frequency of Oscillation kHz	Particle Diameter in Microns	$v_p/v_{0.176}$	
		Experimental	Theoretically Calculated (From Stokes Law)
4.99	0.500	1.00	0.99
4.99	0.760	1.00	0.99
4.99	1.011	1.00	0.99
4.99	2.020	0.88	0.91
20.84	0.500	1.00	0.99
20.84	0.760	0.97	0.96
20.84	1.011	0.92	0.89
20.84	2.020	0.43	0.48
32.15	0.500	1.00	0.98
32.15	0.760	0.90	0.92
32.15	1.011	0.79	0.80
32.15	2.020	0.32	0.33
51.46	0.500	0.90	0.95
51.46	0.760	0.73	0.82
51.46	1.011	0.60	0.64
51.46	2.020	0.19	0.21
84.80	0.500	0.82	0.88
84.80	0.760	0.66	0.65
84.80	1.011	0.45	0.45
84.80	2.020	0.13	0.13

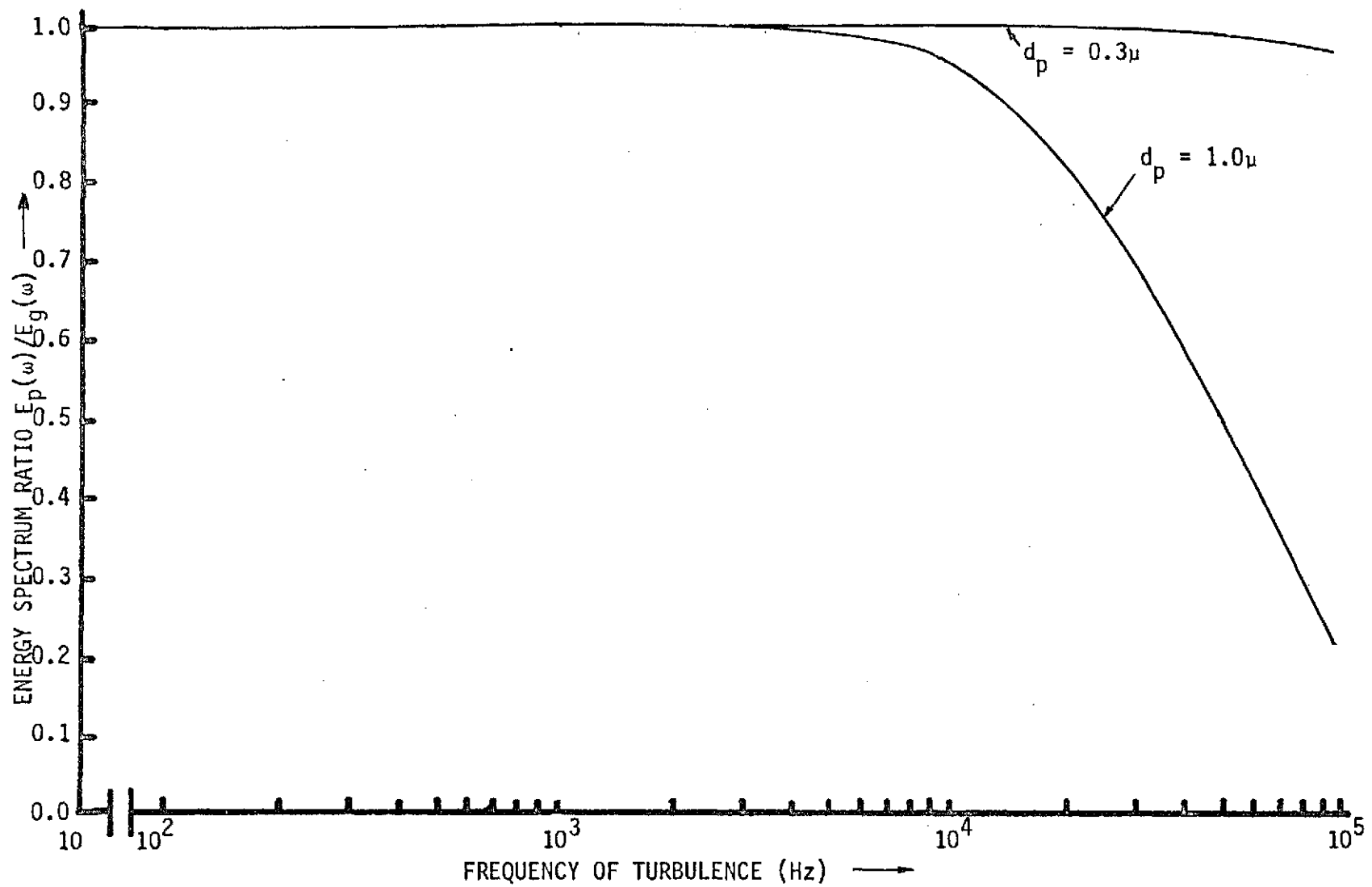


FIGURE 1

DECREASE OF ENERGY SPECTRUM RATIO $E_p(\omega)/E_g(\omega)$ WITH INCREASING
 TURBULENCE FREQUENCY AS A FUNCTION OF PARTICLE SIZE

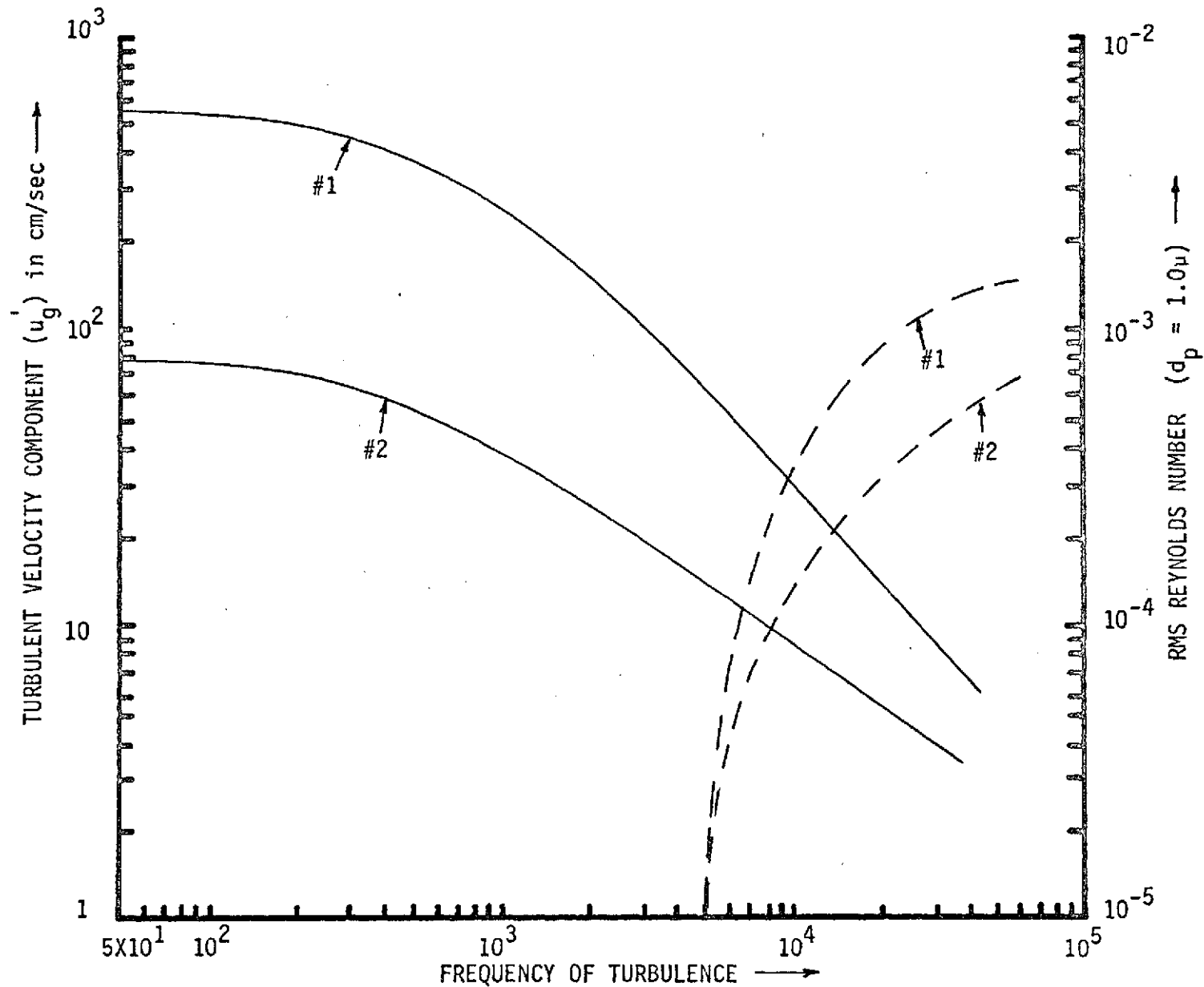


FIGURE 2

TYPICAL RMS TURBULENT VELOCITY COMPONENTS OF SUBSONIC FLUID FLOW IN A WIND TUNNEL ($\bar{U}_0 = 300$ m/sec) AND THE CALCULATED REYNOLDS NUMBER OF A UNIT DENSITY SPHERICAL PARTICLE PLOTTED AS A FUNCTION OF TURBULENCE FREQUENCY

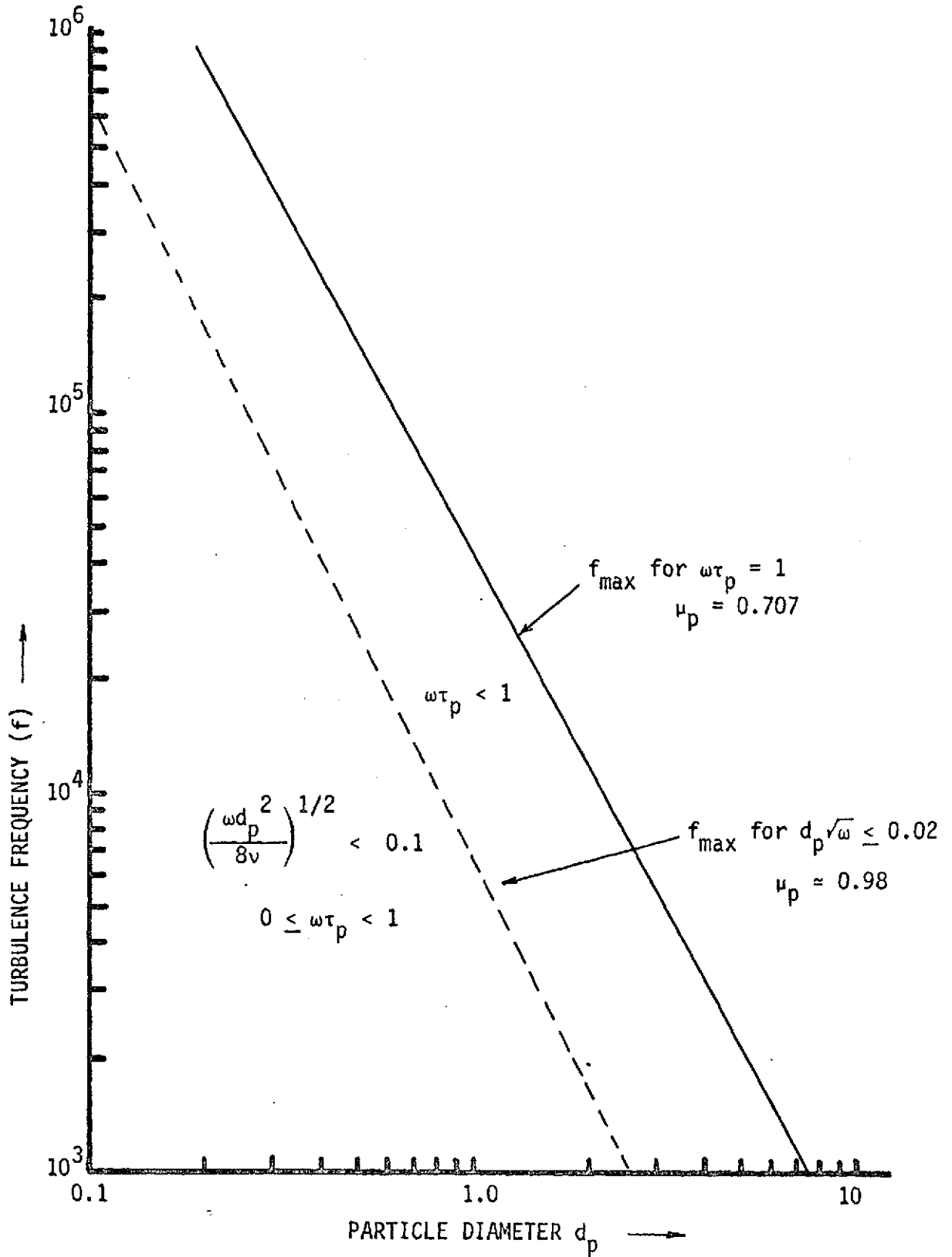


FIGURE 3

MAXIMUM VALUES OF THE TURBULENCE FREQUENCY AND THE DIAMETER OF UNIT DENSITY SPHERICAL SCATTERER FOR TWO ENTRAINMENT FACTORS, $v_p/u_g = 0.707$ or $\omega\tau_p = 1$ and $v_p/u_g = 0.980$ or $d_p\sqrt{\omega} = 0.02$

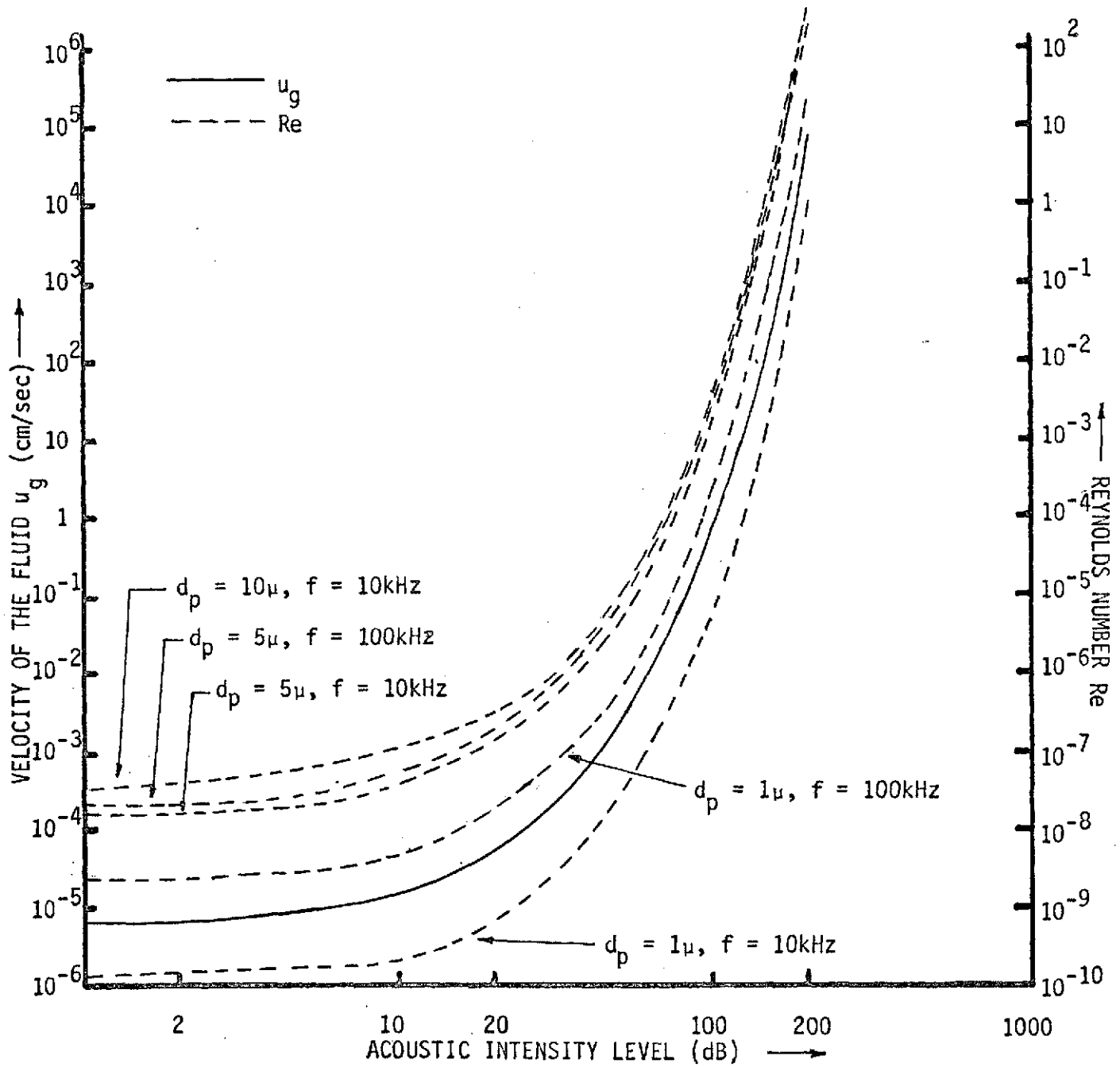


FIGURE 4

CALCULATED VARIATION OF THE FLUID VELOCITY AMPLITUDE (u_g) AND THE ASSOCIATED PARTICLE REYNOLDS NUMBER IN AN ACOUSTIC FIELD PLOTTED AS A FUNCTION OF ACOUSTIC INTENSITY LEVEL

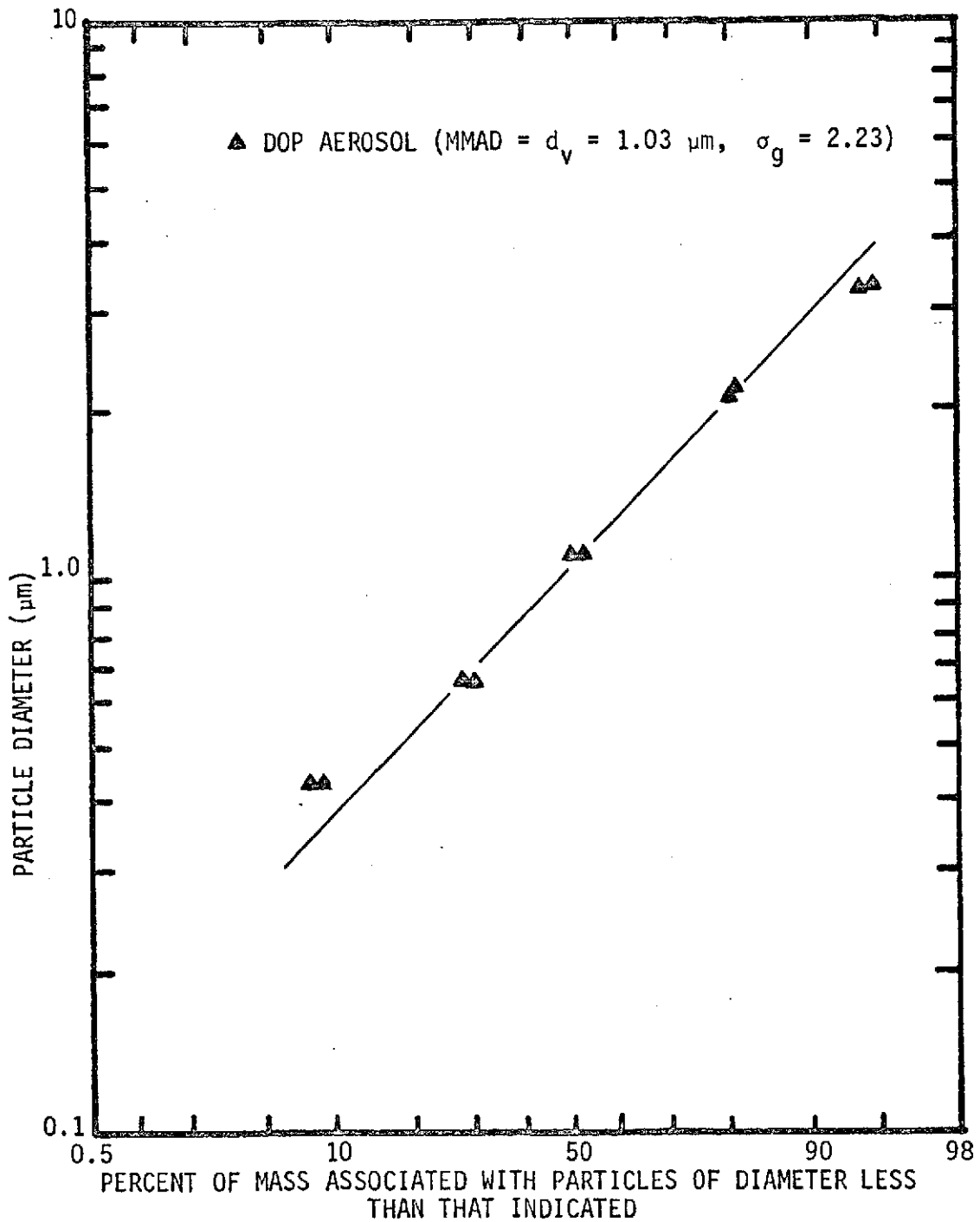
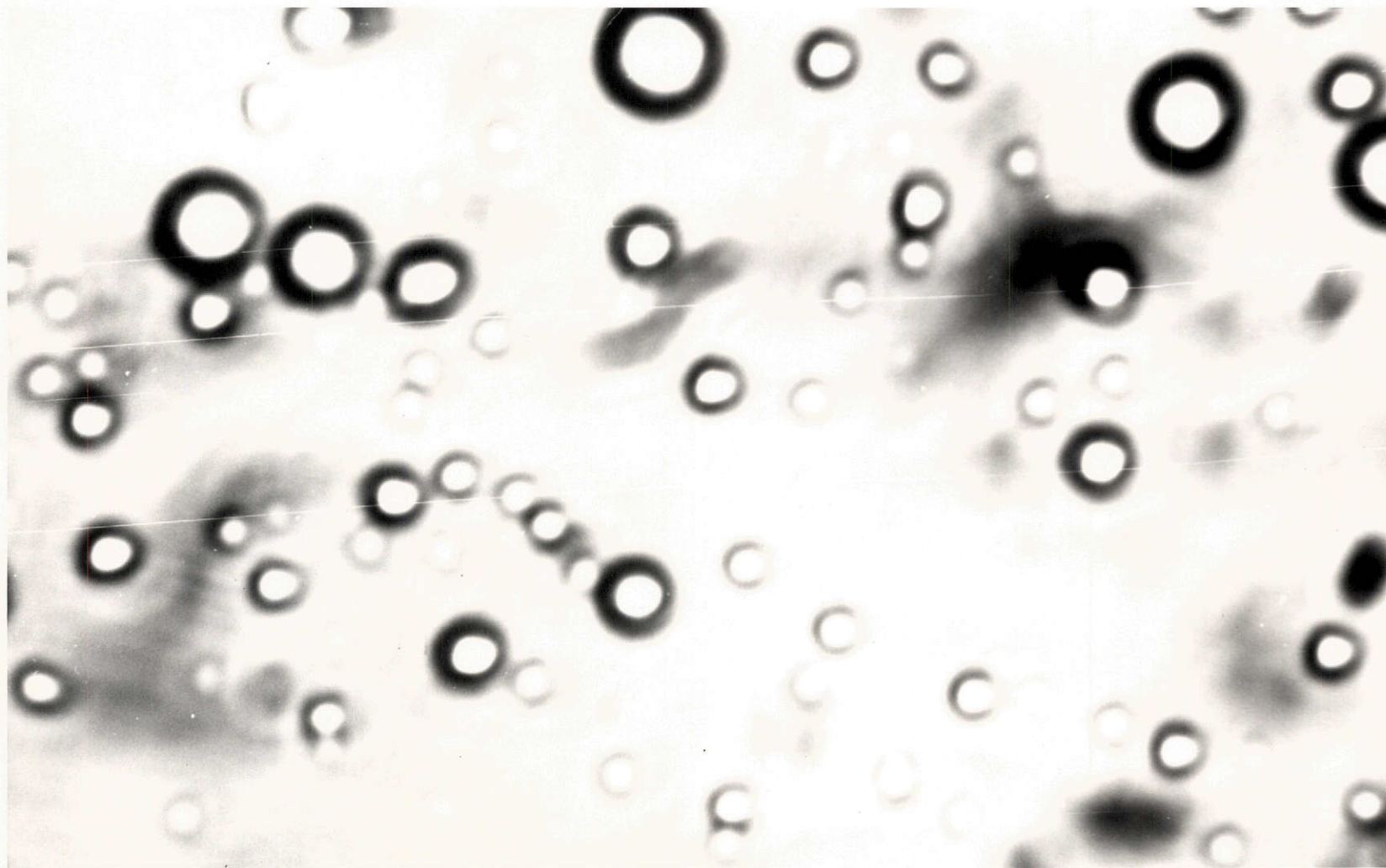


FIGURE 5
CUMULATIVE TYPICAL SIZE DISTRIBUTION CURVE FOR DOP AEROSOL GENERATED BY LASKIN ATOMIZER



30

FIGURE 5A

A PHOTOMICROGRAPH OF DOP AEROSOL GENERATED BY A
LASKIN ATOMIZER (LINEAR MAGNIFICATION = 2090X)

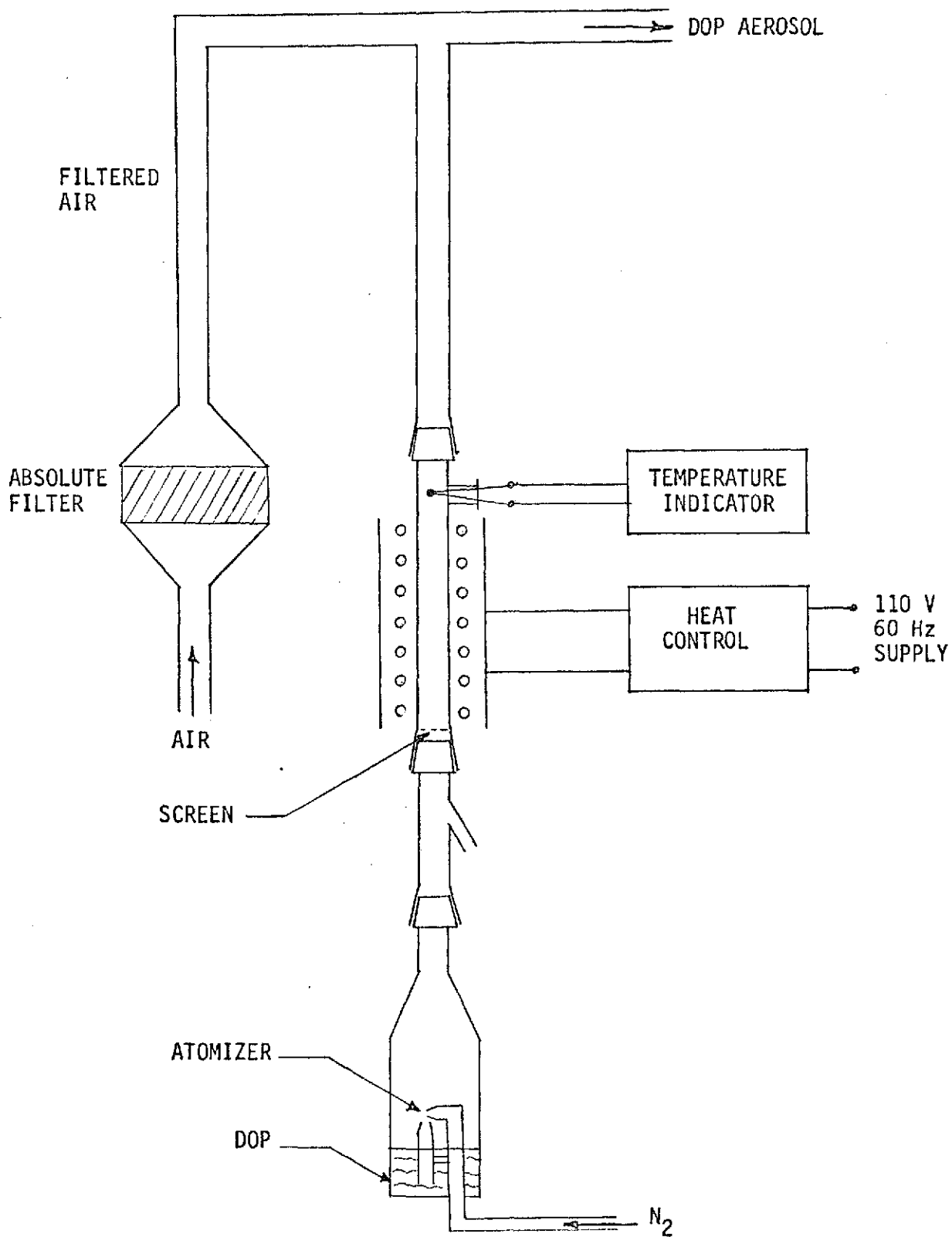


FIGURE 6

RAPAPORT-WEINSTOCK AEROSOL GENERATOR



32

FIGURE 7

A PHOTOMICROGRAPH OF DOP AEROSOL GENERATED BY RAPAPORT-WEINSTOCK GENERATOR USING A 25 PERCENT CONCENTRATION OF DOP (LINEAR MAGNIFICATION = 2090X)



33

FIGURE 7A

A PHOTOMICROGRAPH OF DOP AEROSOL GENERATED BY RAPAPORT-WEINSTOCK
GENERATOR USING A 5 PERCENT CONCENTRATION OF DOP (LINEAR MAGNIFICATION = 2090X)

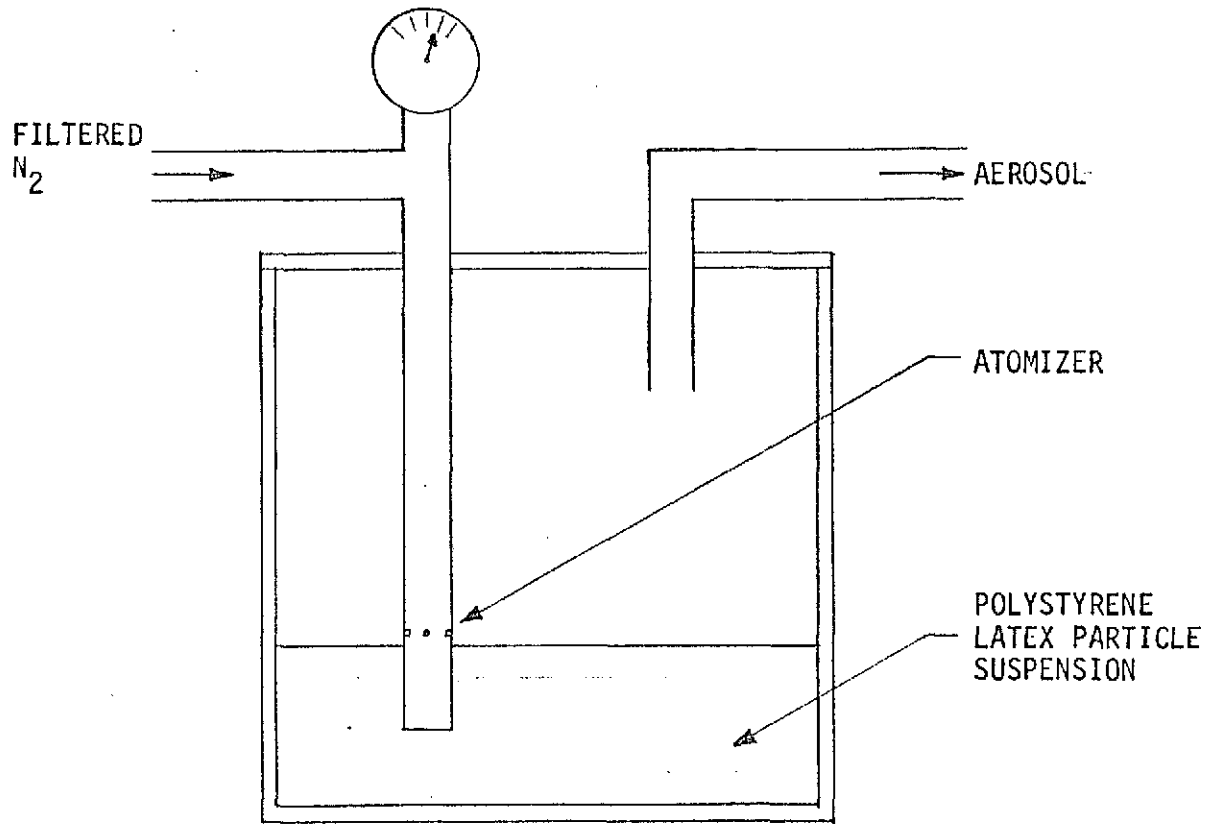
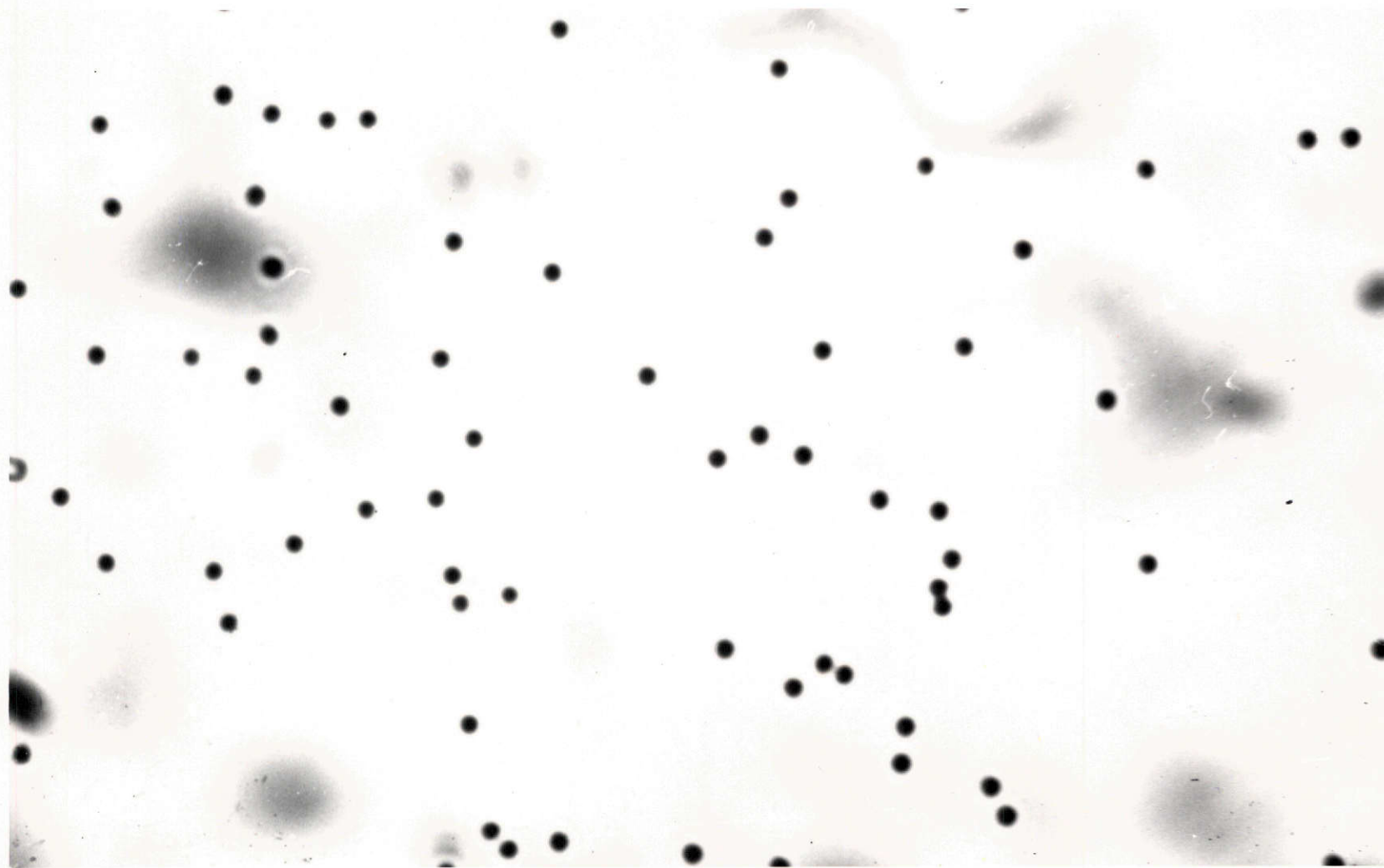


FIGURE 8

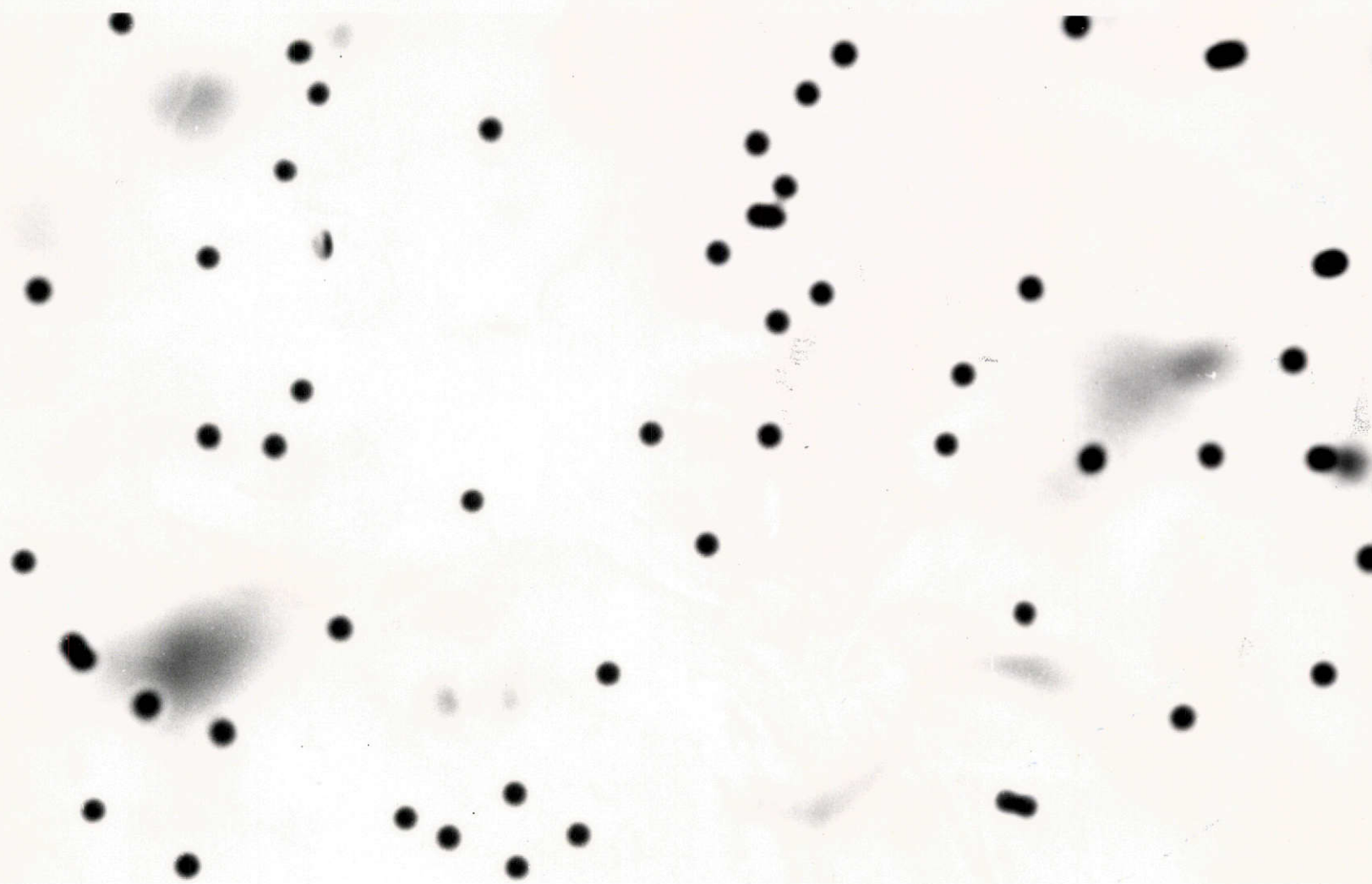
POLYSTYRENE LATEX PARTICLE AEROSOL GENERATOR



-35-

FIGURE 9

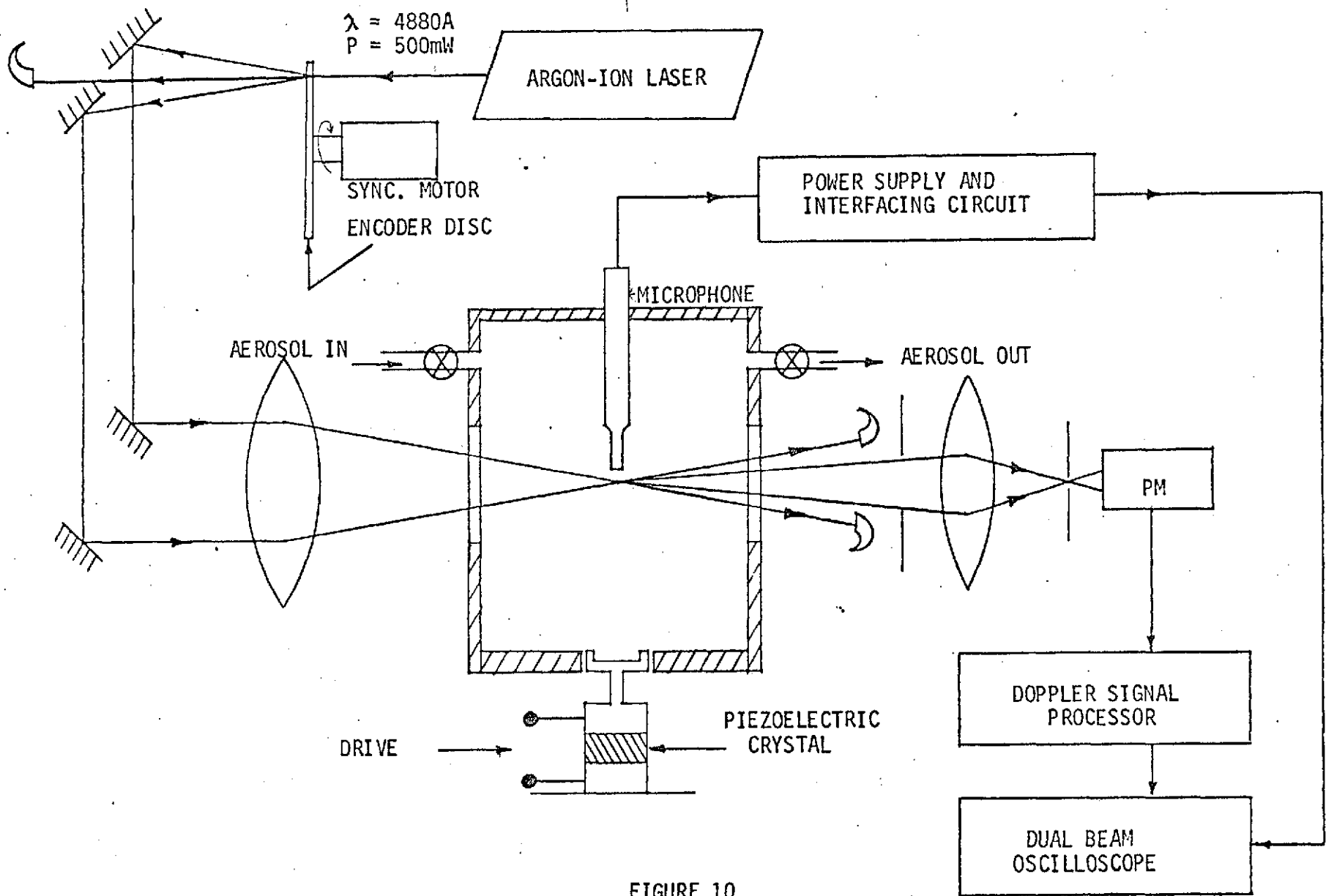
A PHOTOMICROGRAPH OF 0.500 MICRON-DIAMETER POLYSTYRENE
LATEX AEROSOL (LINEAR MAGNIFICATION = 2090X)



-36-

FIGURE 9A

A PHOTOMICROGRAPH OF 1.011 MICRON-DIAMETER POLYSTYRENE
LATEX AEROSOL (LINEAR MAGNIFICATION = 2090X)



-37-

FIGURE 10

AN EXPERIMENTAL ARRANGEMENT FOR MEASURING THE FREQUENCY RESPONSE OF SCATTERING AEROSOL OSCILLATING IN AN ACOUSTIC FIELD

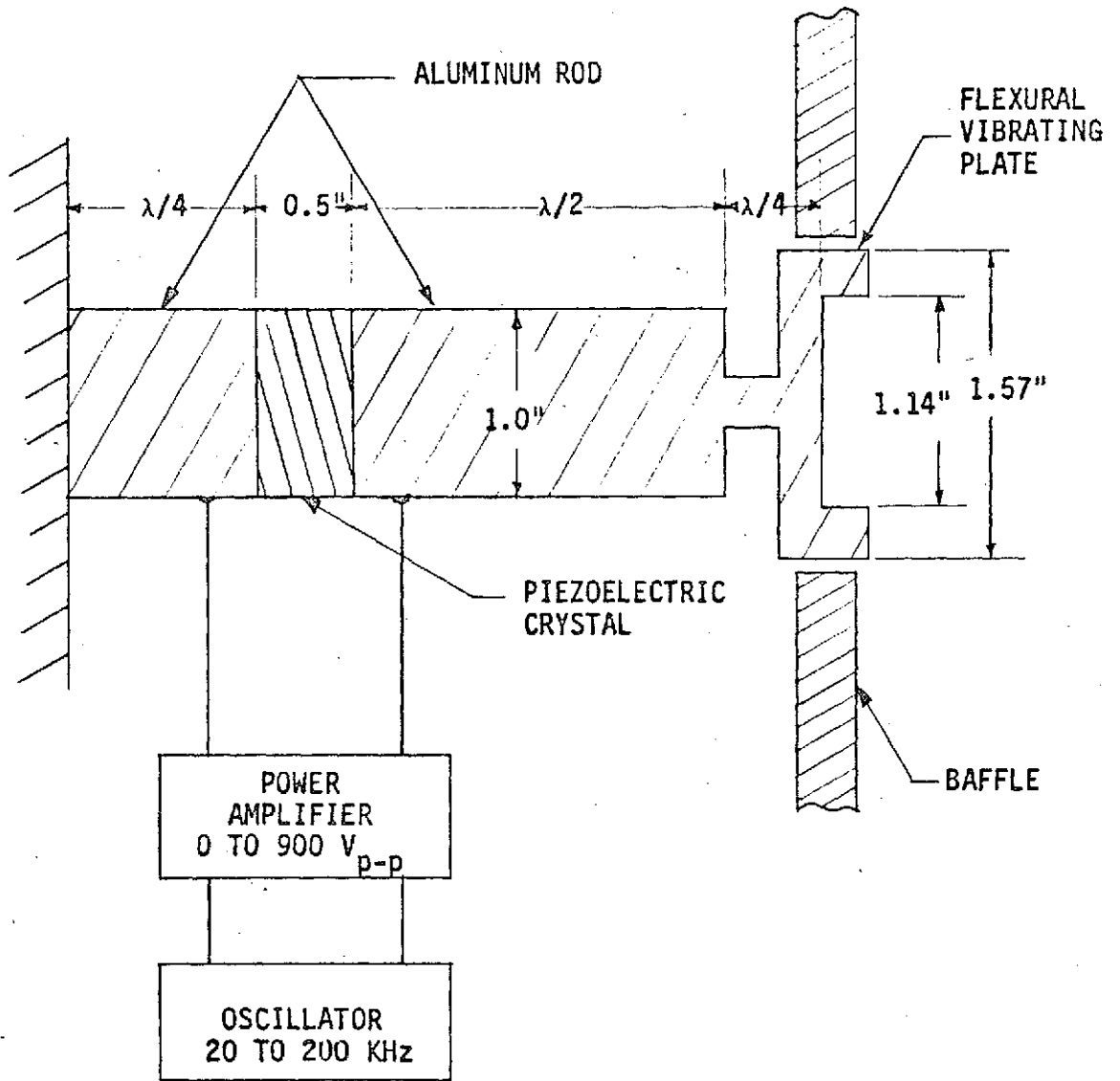


FIGURE 11
SCHEMATIC DIAGRAM OF A CIRCULAR PLATE RADIATOR
(λ = WAVELENGTH OF SOUND IN THE RADIATOR MATERIAL).

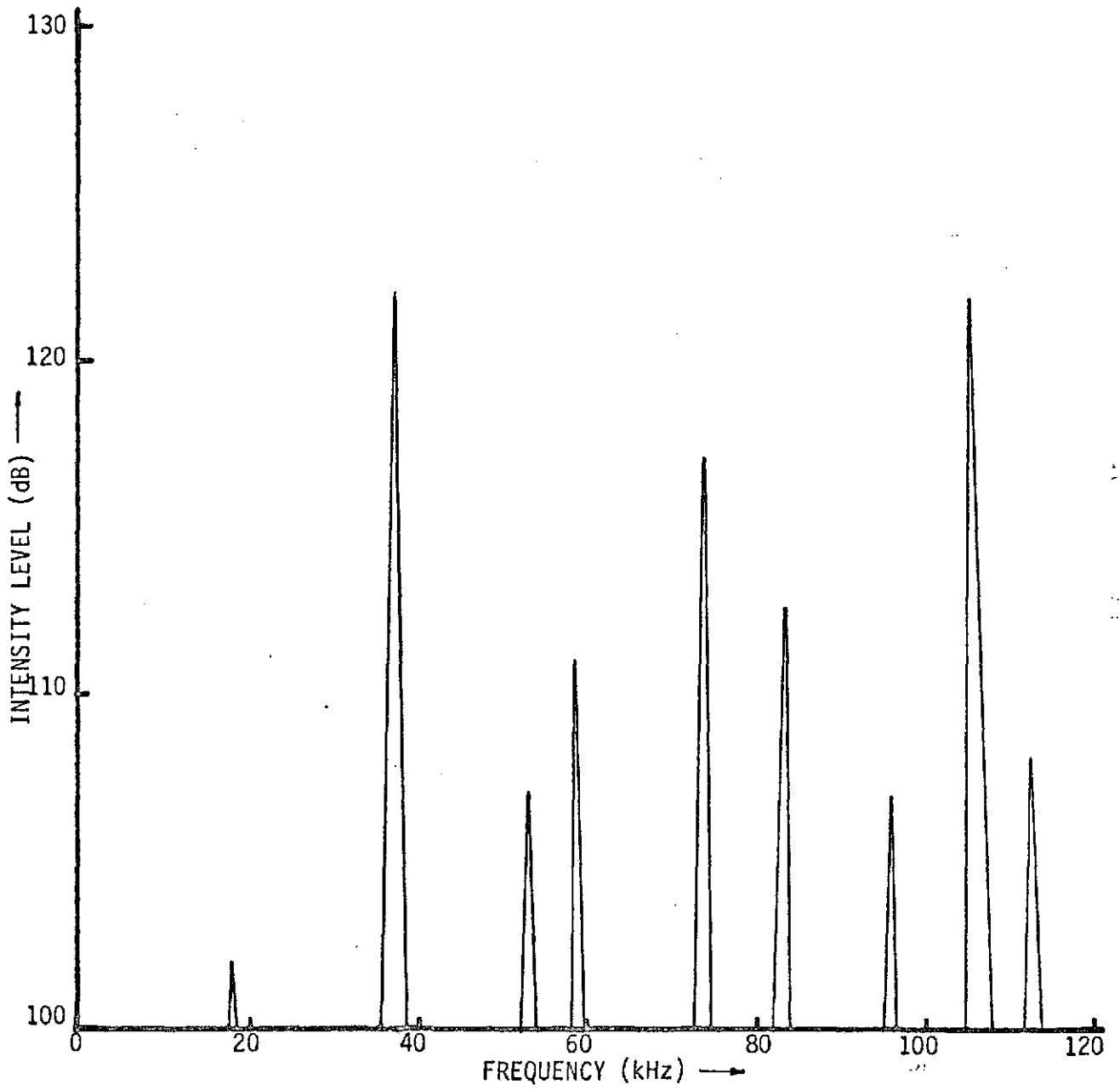
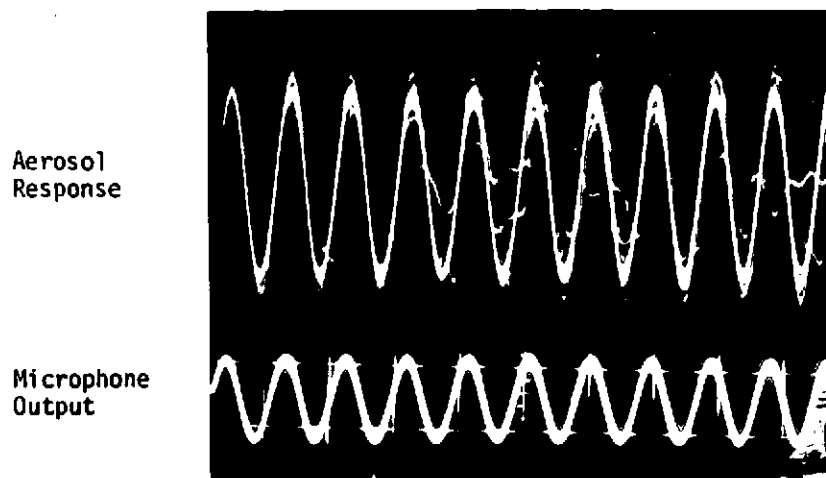
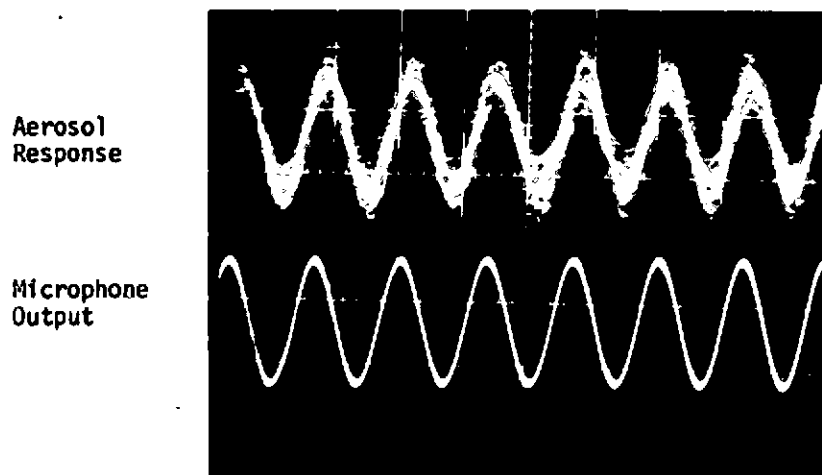


FIGURE 12

ULTRASONIC INTENSITY LEVELS MEASURED AT A DISTANCE OF 3 CENTIMETERS FROM THE TOP OF THE RADIATING PLATE AS A FUNCTION OF EXCITATION FREQUENCY. INPUT VOLTAGE 600 VOLTS PEAK-TO-PEAK, RESONANCE FREQUENCY = 37.8kHz.



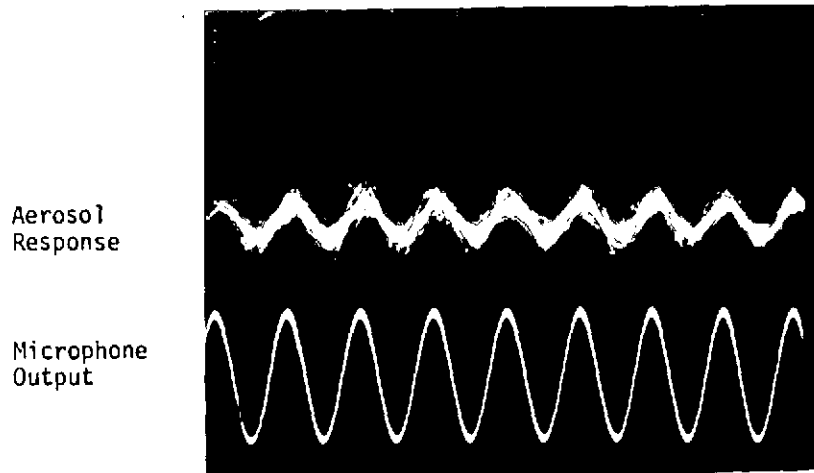
(a) Frequency of Excitation: 4.99 kHz



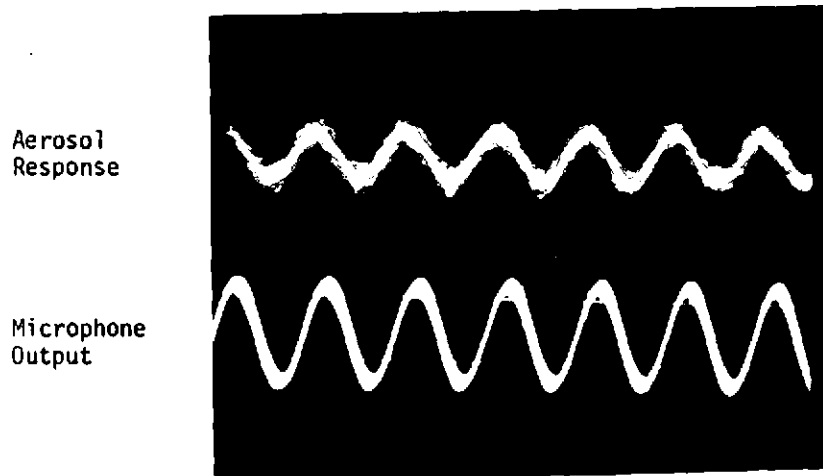
(b) Frequency of Excitation 20.84 kHz

FIGURE 13

RESPONSE OF A POLYDISPERSE DOP AEROSOL ($\sigma_g > 2.0$, AVERAGE DIAMETER 1.03 MICRONS, CONCENTRATION $\approx 10^7$ PARTICLES/cc) IN ACOUSTIC FIELDS



a. Frequency of Excitation: 32.15 kHz



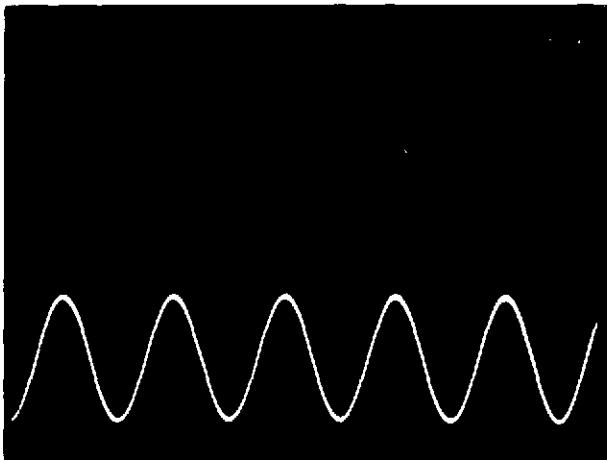
b. Frequency of Excitation: 51.46 kHz

FIGURE 14

RESPONSE OF A POLYDISPERSE DOP AEROSOL ($\sigma_g > 2.0$, AVERAGE DIAMETER 1.03 MICRONS, CONCENTRATION = 10^7 PARTICLES/cc) IN ACOUSTIC FIELDS. PARTICLE SIZE RANGE: 0.3 - 2.0 MICRONS

Aerosol
Response

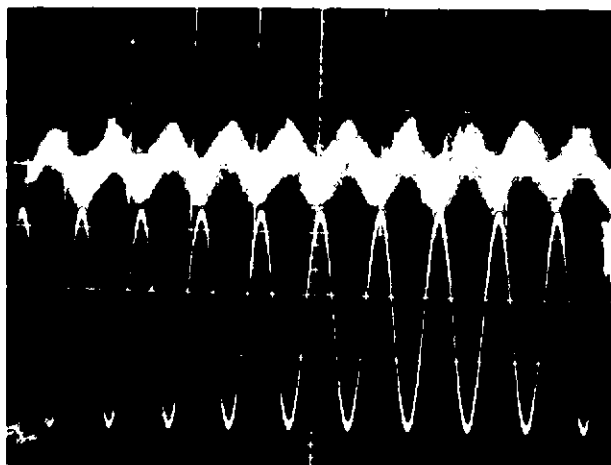
Microphone
Output



a. Frequency of Excitation: 20.84 kHz

Aerosol
Response

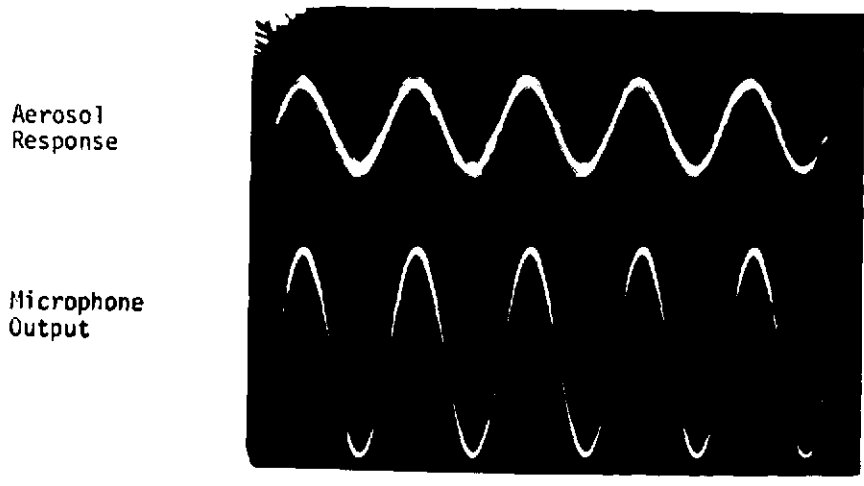
Microphone
Output



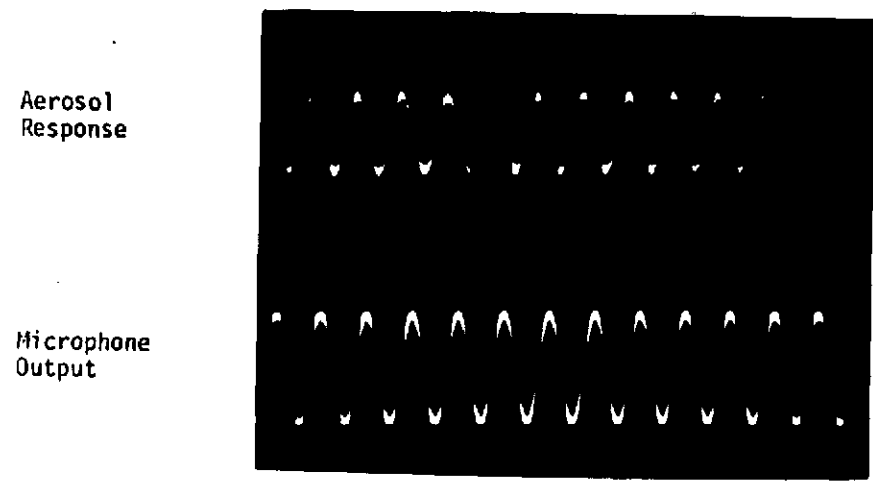
b. Frequency of Excitation: 32.15 kHz

FIGURE 15

POLYDISPERSE DOP AEROSOL RESPONSE IN ACOUSTIC FIELDS MEASURED
BY A DISA 55L20 DOPPLER SIGNAL PROCESSOR



a. Frequency of Excitation: 20.04 kHz



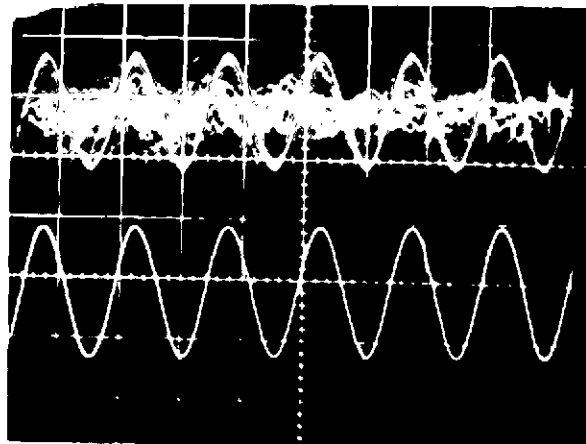
b. Frequency of Excitation: 51.46 kHz

FIGURE 16

FAIRLY MONODISPERSE DOP AEROSOL ($\sigma_g = 1.4$, AVERAGE DIAMETER = 0.6 MICRONS, CONCENTRATION = 10^6 PARTICLES/cc) RESPONSE IN ACOUSTIC FIELDS

Aerosol
Response

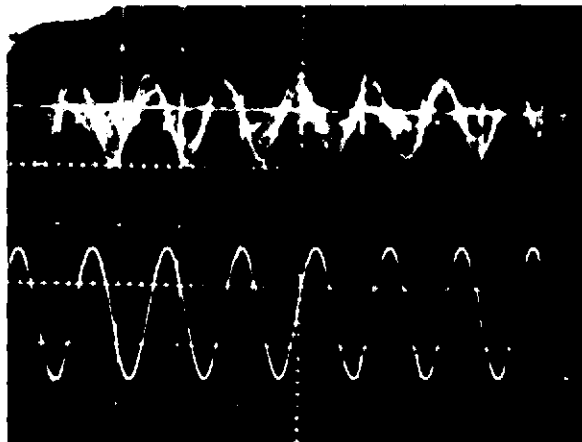
Microphone
Output



a. Frequency of Excitation: 20.84 kHz

Aerosol
Response

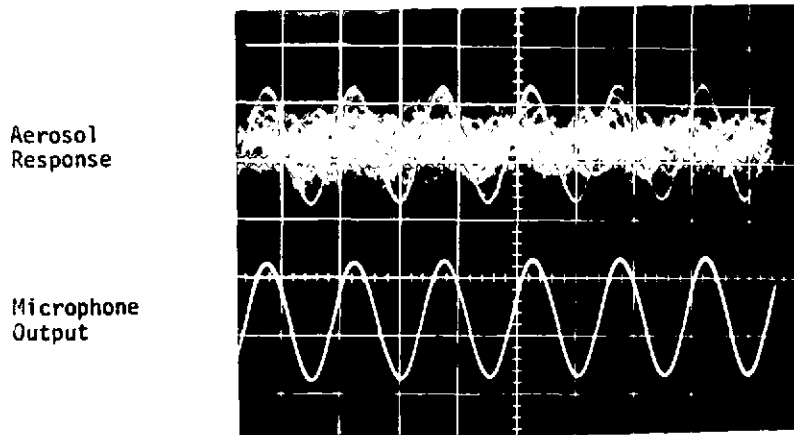
Microphone
Output



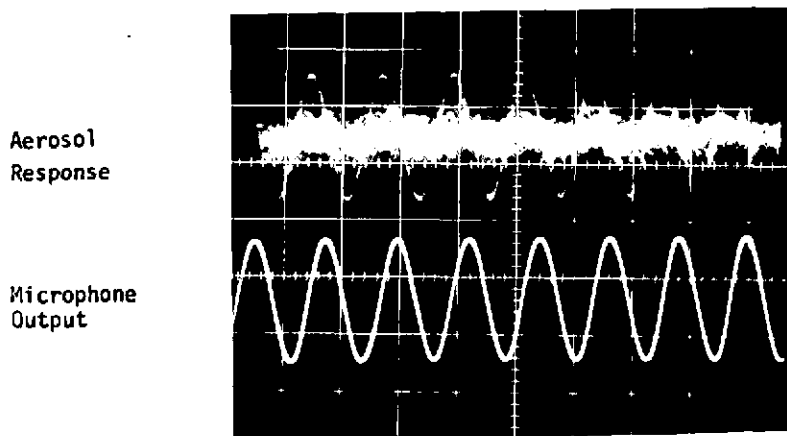
b. Frequency of Excitation: 51.46 kHz

FIGURE 17

MONODISPERSE POLYSTYRENE AEROSOL ($\sigma_g = 1.0$, PARTICLE DIAMETER = 1.01 MICRONS,
CONCENTRATION = 10^5 PARTICLES/cc) RESPONSE IN ACOUSTIC FIELDS



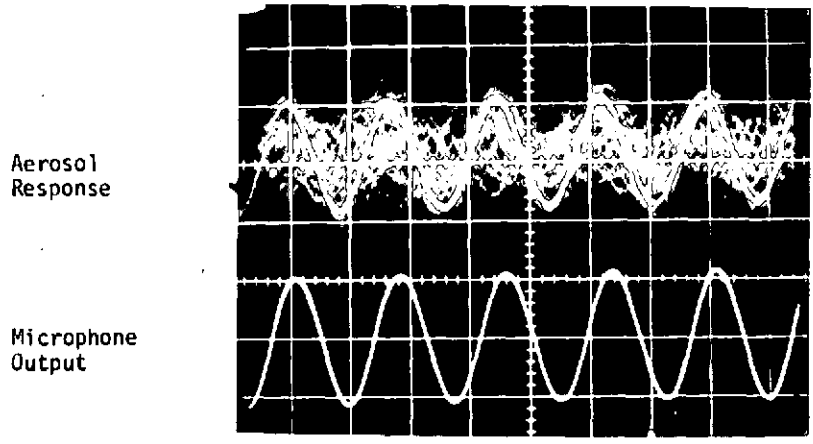
a. Frequency of Excitation: 20.84 kHz



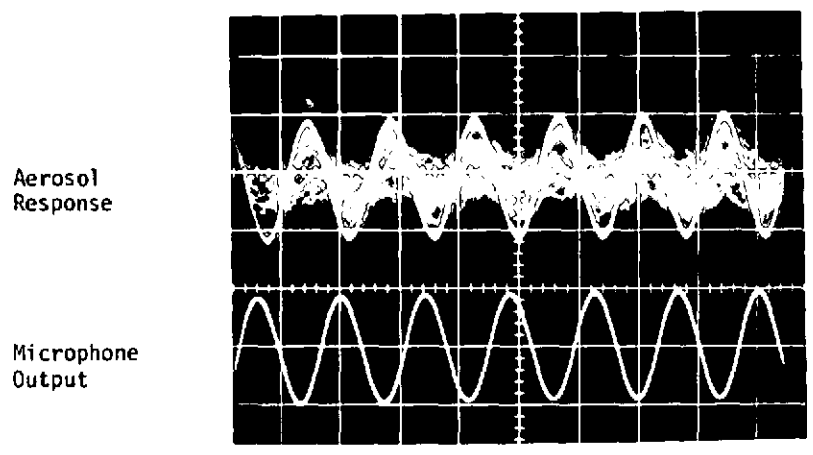
b. Frequency of Excitation: 51.46 kHz

FIGURE 18

MONODISPERSE POLYSTYRENE AEROSOL ($\sigma_g = 1.0$, PARTICLE DIAMETER = 0.50 MICRONS,
CONCENTRATION = 10^5 PARTICLES/cc) RESPONSE IN ACOUSTIC FIELDS



a. Frequency of Excitation: 20.84 kHz



b. Frequency of Excitation: 51.46 kHz

FIGURE 19

MONODISPERSE POLYSTYRENE AEROSOL ($\sigma_g = 1.0$, PARTICLE DIAMETER = 0.17 MICRONS, CONCENTRATION = 10^5 PARTICLES/cc) RESPONSE IN ACOUSTIC FIELDS

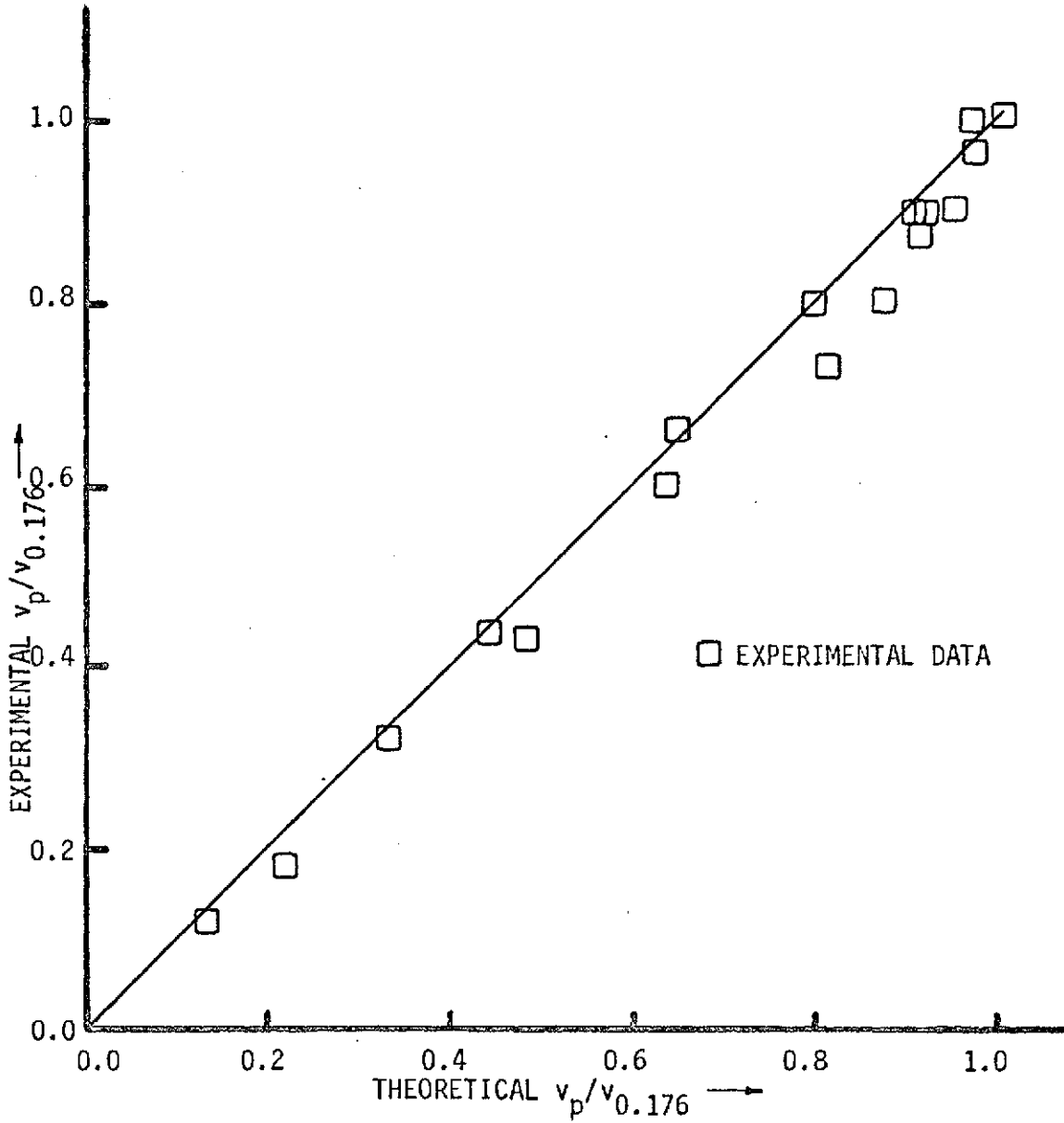
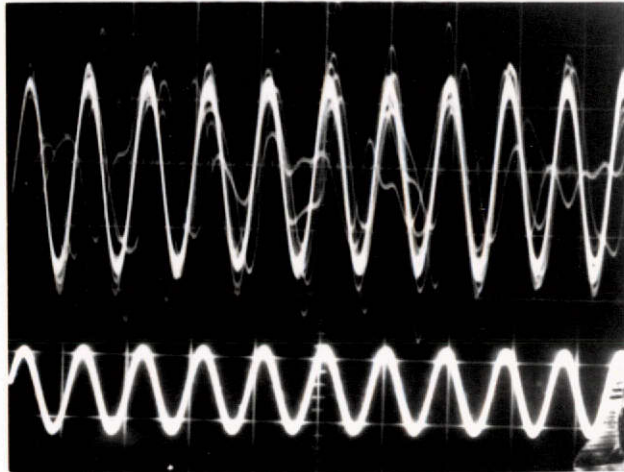


FIGURE 20

COMPARISON OF EXPERIMENTALLY MEASURED AND THEORETICALLY CALCULATED VELOCITY AMPLITUDE RATIOS FOR MONODISPERSE PARTICLES IN THE SIZE RANGE OF 0.176 TO 2.02 MICRON-DIAMETER AND FOR THE FREQUENCY OF OSCILLATION IN THE RANGE 5 TO 85 KHZ

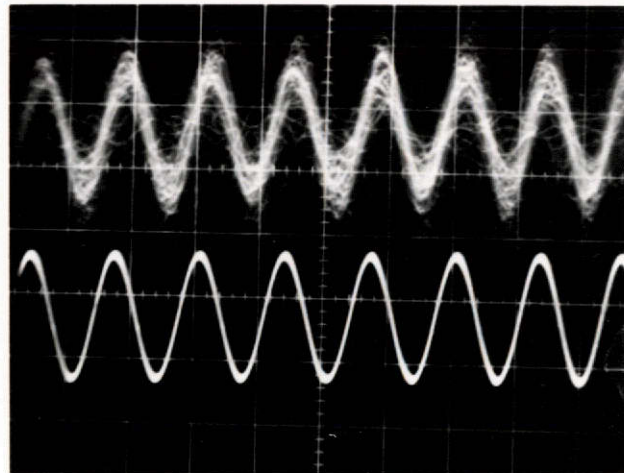
Aerosol
Response



Microphone
Output

(a) Frequency of Excitation: 4.99 kHz

Aerosol
Response

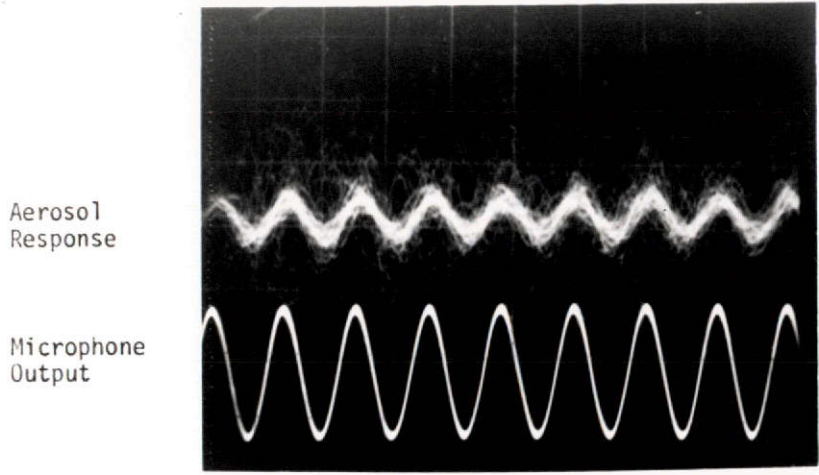


Microphone
Output

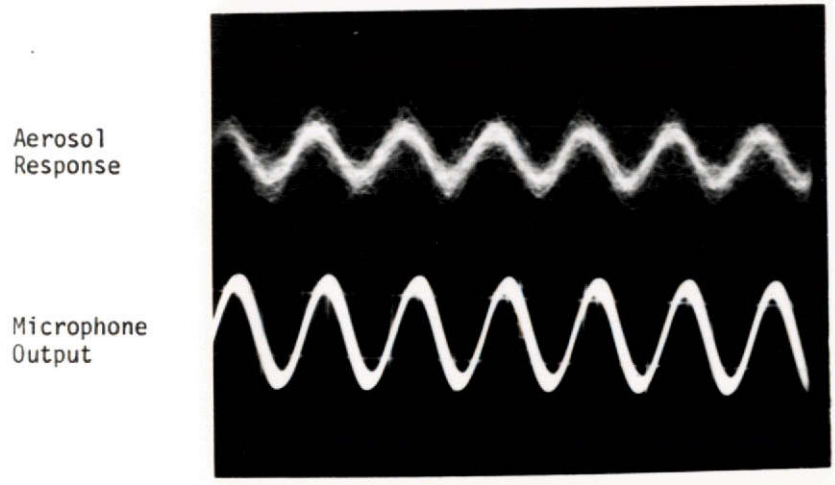
(b) Frequency of Excitation 20.84 kHz

FIGURE 13

RESPONSE OF A POLYDISPERSE DOP AEROSOL ($\sigma_g > 2.0$, AVERAGE DIAMETER
1.03 MICRONS, CONCENTRATION = 10^7 PARTICLES/cc) IN ACOUSTIC FIELDS



a. Frequency of Excitation: 32.15 kHz



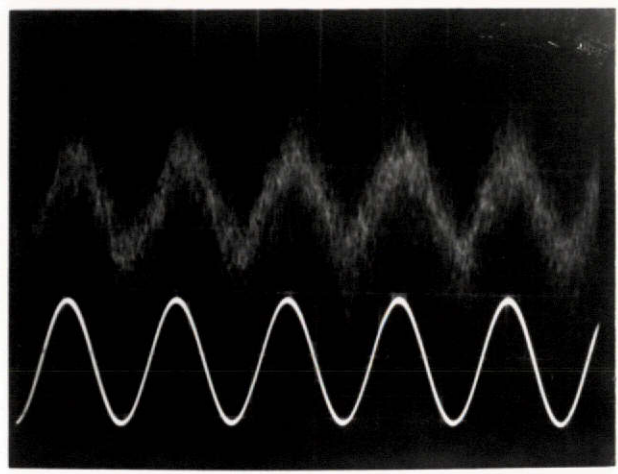
b. Frequency of Excitation: 51.46 kHz

FIGURE 14

RESPONSE OF A POLYDISPERSE DOP AEROSOL ($\sigma_g > 2.0$, AVERAGE DIAMETER 1.03 MICRONS, CONCENTRATION = 10^7 PARTICLES/cc) IN ACOUSTIC FIELDS. PARTICLE SIZE RANGE: 0.3 - 2.0 MICRONS

Aerosol Response

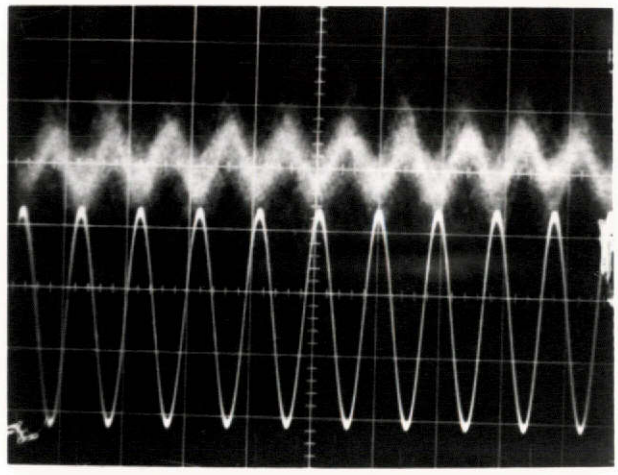
Microphone Output



a. Frequency of Excitation: 20.84 kHz

Aerosol Response

Microphone Output

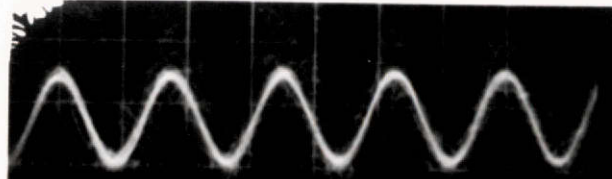


b. Frequency of Excitation: 32.15 kHz

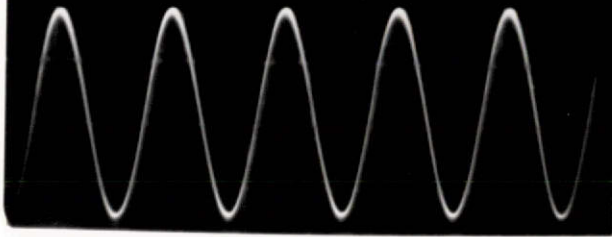
FIGURE 15

POLYDISPERSE DOP AEROSOL RESPONSE IN ACOUSTIC FIELDS MEASURED BY A DISA 55L20 DOPPLER SIGNAL PROCESSOR

Aerosol
Response

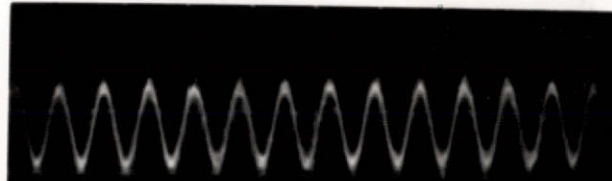


Microphone
Output

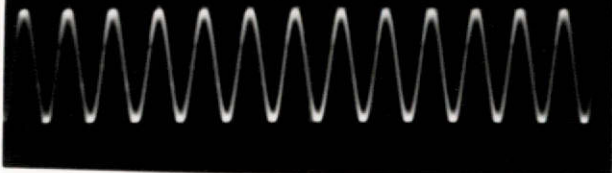


a. Frequency of Excitation: 20.84 kHz

Aerosol
Response



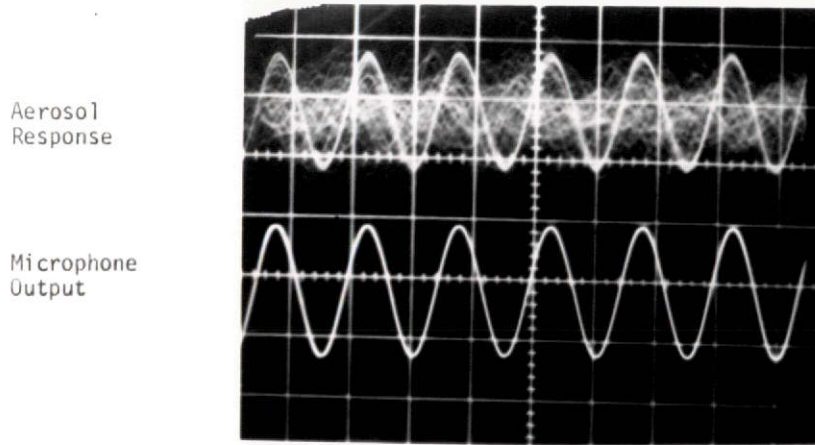
Microphone
Output



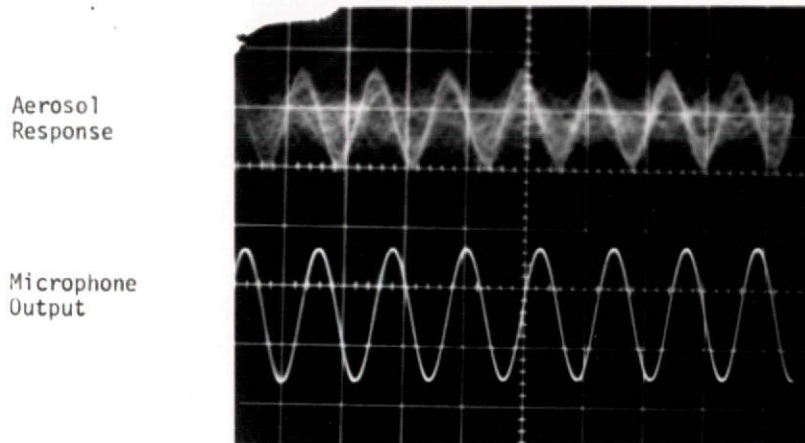
b. Frequency of Excitation: 51.46 kHz

FIGURE 16

FAIRLY MONODISPERSE DOP AEROSOL ($\sigma_g = 1.4$, AVERAGE DIAMETER = 0.6 MICRONS,
CONCENTRATION = 10^6 PARTICLES/cc) RESPONSE IN ACOUSTIC FIELDS



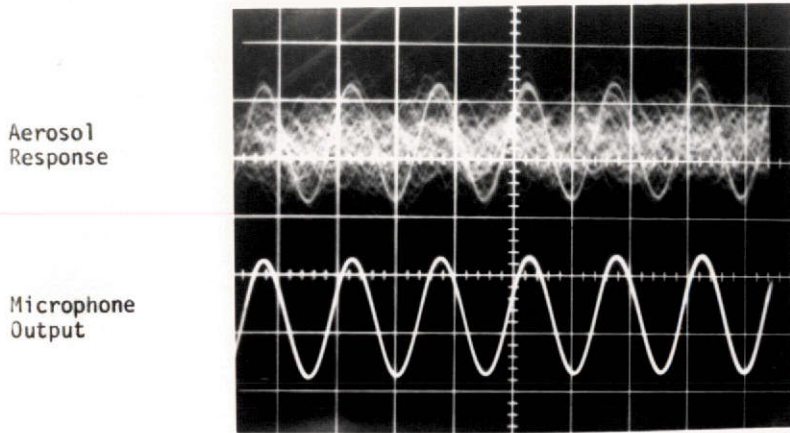
a. Frequency of Excitation: 20.84 kHz



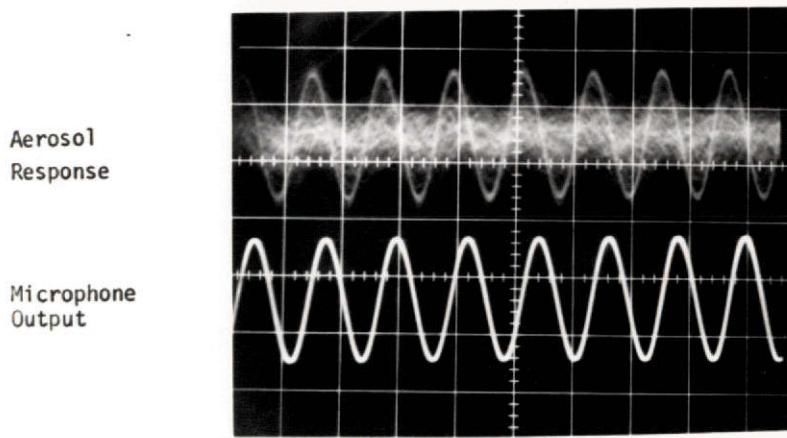
b. Frequency of Excitation: 51.46 kHz

FIGURE 17

MONODISPERSE POLYSTYRENE AEROSOL ($\sigma_g = 1.0$, PARTICLE DIAMETER = 1.01 MICRONS,
CONCENTRATION = 10^5 PARTICLES/cc) RESPONSE IN ACOUSTIC FIELDS



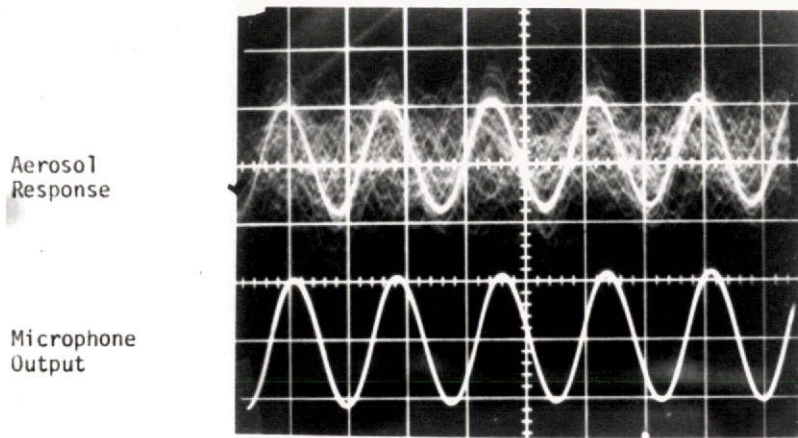
a. Frequency of Excitation: 20.84 kHz



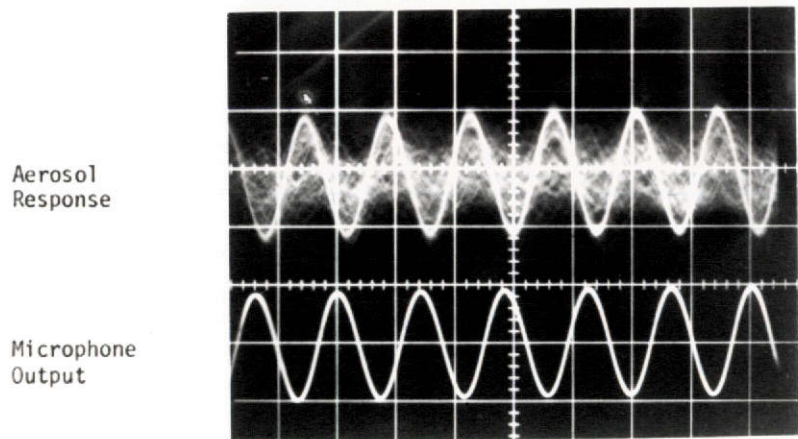
b. Frequency of Excitation: 51.46 kHz

FIGURE 18

MONODISPERSE POLYSTYRENE AEROSOL ($\sigma_g = 1.0$, PARTICLE DIAMETER = 0.50 MICRONS,
CONCENTRATION = 10^5 PARTICLES/cc) RESPONSE IN ACOUSTIC FIELDS



a. Frequency of Excitation: 20.84 kHz



b. Frequency of Excitation: 51.46 kHz

FIGURE 19

MONODISPERSE POLYSTYRENE AEROSOL ($\sigma_g = 1.0$, PARTICLE DIAMETER = 0.17 MICRONS,
CONCENTRATION = 10^5 PARTICLES/cc) RESPONSE IN ACOUSTIC FIELDS